Simulation of Relativistic Electron Rings in Quasi-Equilibrium

I. Hofmann

IPP 0/21 February 1974

MAX-PLANCK-INSTITUT FÜR PLASMAPHYSIK

GARCHING BEI MÜNCHEN

MAX-PLANCK-INSTITUT FÜR PLASMAPHYSIK

GARCHING BEI MÜNCHEN

Simulation of Relativistic Electron Rings in Quasi-Equilibrium

I. Hofmann

IPP 0/21 February 1974

Die nachstehende Arbeit wurde im Rahmen des Vertrages zwischen dem Max-Planck-Institut für Plasmaphysik und der Europäischen Atomgemeinschaft über die Zusammenarbeit auf dem Gebiete der Plasmaphysik durchgeführt.

IPP 0/21 I. Hofmann Simulation of Relativistic Electron Rings in Quasi-Equilibrium

Abstract

An electron ring model and numerical code are developed to describe the quasi-equilibrium behaviour of ion-loaded rings, including inhomogeneous space charge effects and a realistic ion distribution function. The model uses distribution functions that solve the Vlasov equations using appropriate adiabatic invariants. The potentials for electric and magnetic self-fields are calculated in toroidal geometry with a quick 2 D-Poisson solver. Self-consistency is obtained by iterative solution of the resulting coupled nonlinear integro-differential equations. The numerical code is applied to accelerated rings, and the dependence of the holding power on ion loading and close boundaries is studied.

Contents

A. Introduction

The property of a ring of relativistic electrons to produce strong electric fields, which may be used for collective ion acceleration, has been the subject of many investigations in the past few years.

In order to establish performance characteristics for an electron ring accelerator (ERA), one is concerned with instability problems as well as the question of equilibrium state. Instabilities turned out to pose severe limits to the effectiveness of ion acceleration (see D. Möhl, L.J. Laslett, A.M. Sessler (1972)). As far as the equilibrium state is concerned - it is in fact the starting point for instability investigations - models were used in the past which often show substantial lack of selfconsistency from the point of view of the Vlasov equation. Nevertheless the following questions have been attacked by such models: dimensions of an ER after compression and ionization and maximum electric fields in the ring, damping of betatron oscillation amplitudes for electrons and ions during adiabatic changes, inhomogeneous densities in connection with anharmonic betatron oscillations, parameter region (field index, ion loading, electric and magnetic boundary conditions, applied acceleration etc.) in which ring integrity can be maintained, and others. Most of the theoretical work was done along the following lines:

1. Selfconsistent particle codes (J.P. Boris, R. Lee (1971)); with present-day computers they are restricted to the study of short physical times and are unappropriate for adiabatically changing equilibria, as occur during compression and rest-gas-ionization in ERA.

2. Virial theorems (W.H. Kegel (1969), S. Yoshikawa (1972)) and macroscopic fluid models (P. Merkel, (1973)); they relate pressure, density, current and electric and magnetic fields with each other and lead to some macroscopic properties of rings.

3. Non-selfconsistent models based on the Vlasov-equation; selfconsistency is violated by the asumption of electron and ion densities being similar and uniform, which allows only harmonic betatron oscillations with familiar adiabatic invariants (L.J. Laslett (ERAN 30,159), W.A. Perkins (ERAN 97), R.C. Davidson, J.D. Lawson (1972) and others); some authors study nonuniform densities without taking regard of the anharmonic type of particle motion consistent herewith (L.J. Laslett (ERA 19), C. Bovet (ERAN 88)); a more realistic ion distribution function in a ring with uniform eletron density was recently derived by A.A. Drozdovskii (1973); the problem of polarization of an electron-ion-ring during acceleration was treated numerically by N.Yn. Kazarinov, E.A. Perelshtein (1972), using microcanonical distribution functions and approximating ring cross sections by ellipses.

In calculations of electron-ion ring equilibria there are two main problems: 1. choice of a realistic initial equilibrium that solves the Vlasov equation, 2. correct time-dependance of the distribution functions during adiabatic changes. In the framework of equilibrium theory of course initial conditions have to be reguessed whenever an instability that leads to short-time nonequlibrium behaviour of the ring is crossed. Above mentioned papers either violate 1. or 2. and therefore it is desirable to develop an equilibrium model which is free from such simplifications and gives a realistic and trustworthy picture of the nonlinear collective equilibrium behaviour of electron ion rings during compression, ion accumulation and acceleration. The present work attempts such a model in the framework of the Vlasov-Maxwell-equations. It proceeds in the following order: basic equations and assumptions on the distribution functions for stationary equilibria (part B), introduction of adiabatic invariants to describe the time dependance of distribution functions in times which are long compared to betatron oscillation times (part C) and finally a numerical code, which solves the resulting nonlinear integro-differential-equations with different boundary conditions. The code will be applied to the principal equilibrium problems occurring in ERA (part E).

B. Stationary Vlasov Equilibria for an Electron Ring with Ions

Particles in a ring of relativistic electrons and ions execute betatron oscillations transverse to the azimuthal direction. They are subjected to forces which may arise from an external magnetic mirror or homogeneous guiding field, from selffields of the ring, from currents and charges on surrounding structures and from additional fields necessary to accelerate or stabilize the ring. If the transverse oscillations are predominantly controlled by an external focusing field, the frequently used single-particle picture of orbits in a prescribed field is convenient. In a regime, where electrons and ions are mainly confined by the field produced by themselves, i.e. a pronounced collective behaviour, a Vlasov description is appropriate. This will be the framework of the present paper.

I. Basic Equations

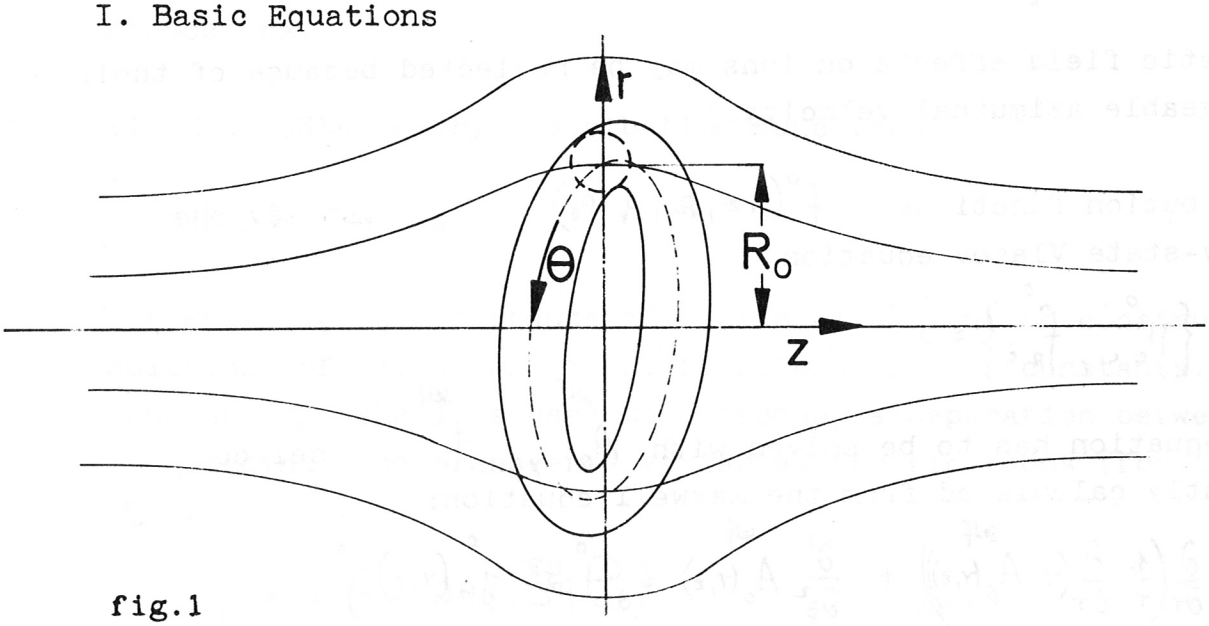

fig.1

Electrons and ions are assumed to be uniformly distributed in azimuthal direction. In this direction electrons shall have relativistic velocities. The motion of electrons is governed by the relativistic Hamiltonian

$$(1)\quad H_e^o = \left(m_o^2 c^4 + c^2 \vec{p}^2\right)^{1/2} - e\,\phi_o(r,z) \quad , \quad \frac{\partial H_e^o}{\partial \theta} = 0$$

with $\underset{\rightarrow}{P} = \{P_r, P_z, P_\theta\}$ and canonical momenta

$$P_r = p_r \,, \quad P_z = p_z \,, \quad P_\theta = r\left(p_\theta - \frac{e}{c} A_0(r,z)\right) \,, \quad \dot{P}_\theta = 0$$

and particle velocities

$$\underset{\rightarrow}{V} = \frac{\underset{\rightarrow}{P}}{m_0\left(1+\underset{\rightarrow}{P}^2/m_0^2c^2\right)^{1/2}}$$

A_0 is the θ-component of the vector potential for total magnetic field $\underset{\rightarrow}{B}_0^{ext} + \underset{\rightarrow}{B}_0^{self}$ and ϕ_0 the scalar potential $\phi_0^{ext} + \phi_0^{self}$.

For ions the nonrelativistic Hamiltonian is

$$(2) \quad H_i^0 = \frac{\underset{\rightarrow}{P}^2}{2m_i} + e\,\phi_0(r,z)$$

(magnetic field effects on ions may be neglected because of their negligeable azimuthal velocity.)

Distribution functions $f^0(r,z,p_r,p_z,p_\theta)$ satisfy the steady-state Vlasov equation

$$(3) \quad \left\{H_{e,i}^0 \,,\, f_{e,i}^0\right\} = 0$$

This equation has to be solved with A_0^{self}, ϕ_0^{self} selfconsistently calculated from the Maxwell equation:

$$(4) \quad \frac{\partial}{\partial r}\left(\frac{1}{r}\frac{\partial}{\partial r}\left(r\,A_0^{self}(r,z)\right)\right) + \frac{\partial^2}{\partial z^2} A_0^{self}(r,z) = -\frac{4\pi}{c}\, j_\theta^0(r,z)$$

and Poisson equation

$$(5) \quad \frac{1}{r}\frac{\partial}{\partial r}\left(r\frac{\partial}{\partial r}\,\phi_0^{self}(r,z)\right) + \frac{\partial^2}{\partial z^2}\,\phi_0^{self}(r,z) = 4\pi e\left(n_e^0(r,z) - n_i^0(r,z)\right)$$

with

$$(6) \quad n_{e,i}^0(r,z) \equiv \frac{1}{2\pi r}\int d^3p\; f_{e,i}^0\left(r,z,p_r,p_z,p_\theta\right)$$

(7) $$j_\theta^0(r,z) \equiv e\, n_e^0(r,z)\, v_\theta^0(r,z) \equiv e\int d^3p\, v_\theta\, f_e^0$$

and the total particle number

$$N_{e,i} = \int dr\, dz\, d^3p\, f_{e,i}^0(r,z,p_r,p_z,p_\theta)$$

Since current- and charge densities nonlinearly depend on the potentials via integrals over the distribution functions, equations (1-7) represent nonlinear integro-differential-equations

(8) $$L^* A_0^{self} = J(A_0, \phi_0)^{self}$$

(9) $$L\, \phi_0^{self} = Q(\phi_0^{self}, A_0^{self})$$

Boundary conditions are to be posed at infinity or on finite conductors.

II. Exact Stationary Distribution Functions

1. General Remarks

The knowledge of constants of motion allows one to construct solutions of (3) as arbitrary functions of such constants. The constant P_θ shall be used to introduce a separation between longitudinal and transverse variables for electrons (for ions let P_θ be zero):

(10) $$f^0 = f_\perp^0(r,z,p_r,p_z)\, g^0(P_\theta) \quad , \text{ where}$$

$g^0(P_\theta)$ prescribes a momentum spread, typically of the order of 5 - 10% for ERA applications. Another constant is the total energy $H_{e,i}^0$, which plays a central part in this work. In fact, other authors have used δ-functions in P_θ, H^0 (see Davidson & Lawson (1972), Kazarinov & Perelshtein (1972)), and thus obtain uniform charge and current densities inside a sharp boundary.

Such a specialization to microcanonical distributions will be avoided in this work, because particles are injected into ER compressors with a Gauß-distribution rather than a δ-distribution, which gives rise to nonlinear effects. Recently an analytic approach to a Gibbs distribution of energy for a stationary ring was made by R.C. Davidson, S.M. Mahajan (1972).

Whether it is sufficiently general to take as transverse distribution function $f_\perp^\circ$ a function of H° alone (even an arbitrary function), is a question of basic importance and will be discussed in the following sections and in chapter C. In fact there may occur various situations, depending on the nature of the Hamiltonian H° governing the transverse motion. It is clear that if besides H° another constant of motion exists, it should be included in the construction of distribution functions to obtain the most general class of such functions. Such additional constants exist, if the Hamiltonian is separable as a function of some appropriately chosen variables. If, for example, the ring would be cut and stretched to a straight beam of infinite length and the potentials A_0, ϕ_0 were rotationally symmetric in the (r, z)-plane, the angular momentum of such rotations would be the second constant of motion. Such a possibility, however, fails for electron rings, because the radial centripetal forces break symmetry between r and z; except for a ring in an applied magnetic mirror field at field index $n = 0.5$, where radial and axial restoring forces are equal.

The possibility of a further, approximate, constant of transverse electron motion for not too strong selffields will be discussed in section C IV.

2. Distributions Uniform on Energy Surfaces

If H° is the only constant of transverse motion known, general stationary distribution functions are, including separation according to (10)

(11) $f_e^0(H_e^0, P_\theta) = f_{e\perp}^0(H_e^0)\, g_e^0(P_\theta)$ and

(12) $f_i^0(H_i^0)$ for ions, i.e. distributions uniform on energy surfaces.

For convenience g_e^0 is chosen as a step function introducing a momentum spread $\frac{\Delta P_\theta}{P_\theta}$

For a given value of P_θ, an equilibrium radius $R(P_\theta)$ and corresponding minimum energy $E_{e\,min}$ are given for electrons according to the following variational principle

(13) $$\delta\left(H_e^0(r, z, p_r, p_z, P_\theta)\right) = 0$$
$$p_r = p_z = 0,\quad -\infty \leq z \leq \infty,\quad 0 < r < \infty$$

Assume the above variational principle yields a minimum at $z = \bar{z}$; the corresponding r value shall be $R(P_\theta)$ and the energy $E_{e\,min}(P_\theta)$. $f_{e\perp}^0$ is then a function which is positive for $E_{e\,min} \leq H_e^0 \leq E_{e\,max} < \infty$ and zero elsewhere.

$f_i^0(H_i^0)$ is a positive function for $E_{i\,min} \leq H_i^0 \leq E_{i\,max} < \infty$ which depends on some ionization equation to be established later on, and on f_e^0 through equations (5),(6).

III. Decoupling of Transverse and Longitudinal (Azimuthal) Energy

Since in ER-applications the "transverse" energy $(E_{e\,max} - E_{e\,min})$ is nonrelativistic, it is usual to expand the square root in H_e^0 (1) and derive a purely transverse Hamiltonian which has nonrelativistic structure. For numerical applications it is convenient to define a zero order equilibrium radius R_0 without self-fields and treat deviations herefrom as perturbations. From (1) follows in this case for B_0^{ext} symmetric in z:

(14) $$\frac{\partial}{\partial r} P_\theta^2 = 2 P_\theta \left(-\frac{P_\theta}{R_0^2} + \frac{e}{c}\frac{\partial A_0^{ext}}{\partial R_0}\right) = 0$$

(15) $$H_e^0 = \left(m_0^2\gamma_0^2 c^4 + 2c^2 P_{\theta_0}\,\delta\left(\frac{P_\theta}{r} + \frac{e}{c}(A_0^{ext} + A_0^{self})\right) + c^2(p_r^2 + p_z^2)\right)^{1/2} - e\,\phi_0^{self}$$
$$= m_0\gamma_0 c^2 + \frac{p_r^2 + p_z^2}{2 m_0 \gamma_0} + V_{\theta_0}\left[\left(\frac{P_\theta}{R_0^3} + \frac{e}{c}\frac{1}{2}\frac{\partial^2 A_0^{ext}}{\partial r^2}\right)\delta r^2 + \frac{e}{c}\frac{1}{2}\frac{\partial^2 A_0^{ext}}{\partial z^2}\delta z^2 + \frac{e}{c}A_0^{self}\right] - e\,\phi_0^{self}$$

(16) $$\gamma_0 \equiv \left(m_0^2 c^4 + c^2 \left(\frac{P_\theta}{R_0} + \frac{e}{c} A_0^{ext}(R_0, 0) \right)^2 \right)^{1/2} / m_0 c^2$$

$V_{\theta_0} \equiv p_{\theta_0} / m_0 \gamma_0$ (azimuthal velocity of a merely gyrating particle with canonical angular momentum P_θ)

$$V_{\theta_0}^2 = 1 - 1/\gamma_0^2$$

where it is assumed that higher derivatives of $\frac{P_\theta}{r} + \frac{e}{c} A_0^{ext}$ than second order are negligeable compared with selffield effects that vary over small distances for densitites high enough. Thus

(17) $$H_{e\perp}^0 = \frac{p_r^2 + p_z^2}{2 m_0 \gamma_0} + \frac{m_0 \gamma_0 V_{\theta_0}^2}{2 R_0^2} \left((1-n) \delta r^2 + n \delta z^2 \right) + \frac{e}{c} V_{\theta_0} A_0^{self} - e \phi_0^{self}$$

with $$n \equiv -\frac{R_0}{B_{0z}} \frac{\partial B_{0z}}{\partial R_0}$$

$$B_r = \frac{\partial A_0}{\partial z}, \quad B_z = \frac{A_0}{r} + \frac{\partial A_0}{\partial r}, \quad \frac{\partial B_{0z}}{\partial r} = \frac{\partial B_{0r}}{\partial z}$$

$$\frac{m_0 \gamma_0 V_{\theta_0}}{R_0} = \frac{e}{c} B_{0z}(R_0, 0)$$

$H_{e\perp}^0$ prescribes classical motion of an electron with mass $m_0 \gamma_0$ in a potential t rough. In the stationary case $H_{e\perp}^0$ is a constant and the nonlinear features of A_0^{self}, ϕ_0^{self} will in general destroy symmetry of the potential and therefore prohibit the existence of a further constant of motion comparable to the energy. Similar to II.2 uniform distributions over surfaces $H_{e\perp}^0 \equiv$ const. in the phase space $\{p_r, p_z, \delta r, \delta z\}$ are the most general explicitly known exact stationary solutions to the Vlasov equation. It should be observed that the zero order radius R_0 is shifted by the selffields $\left(\frac{\Delta R_0}{R_0} > 0\right)$, the direction of the shift depending on boundary conditions.

C. Adiabatic Processes

In part B the functional form of stationary distributions in phase space has been established for the case when besides energy no further constant of (transverse) motion exists. It is clear that during the history of an ER nonstationary processes occur. The instability part of them is beyond the purpose of this work, whereas slow changes of parameters will be considered in the following. Such changes are called adiabatic, if they occur in times sufficiently long as to guarantee reestablishment of (quasi-) equilibrium, i.e. strongly nonstationary phenomena like filamentation of occupied phase space regions should not occur. The question arises, how the phase space flow related to adiabatic changes can be described in terms of distribution functions.

I. Discussion of Nonlinear Effects upon Quasistationary Phase Space Flow

If one starts with a uniform distribution on an energy surface, one may ask whether or not equidistribution will be maintained during a slow change of external parameters. To answer this question, an insight into the dynamical behaviour of orbits for general two dimensional oscillations governed by a Hamiltonian is required.

$$(18)\quad H = \frac{p_r^2 + p_z^2}{2m} + \frac{k_r}{2} r^2 + \frac{k_z}{2} z^2 + \varepsilon \lambda(r,z)$$

It is clear that because of nonuniform space charges potentials occurring in the Hamiltonian (17) will in general be anharmonic, in particular introduce coupling between the two degrees of freedom (r,z), as expressed by $\varepsilon \lambda(r,z)$, (18). For a restricted class of functions $\lambda(r,z)$ H may be separable; in this case a complete integration of the dynamical problem is possible and the resulting integrals of motion define invariant sections on an energy surface H = const. Orbits are restricted to such invariant sections. If the Lebesgue measure of such a subsection is nonzero (exclude the trivial case of measure 1) the energy surface

is metrically decomposable. Since metrical indecomposability is equivalent to ergodicity (see for example Arnold and Avez, 1967), such a flow will be nonergodic. Therefore an extended class of stationary distribution functions will be admitted, including such functions which assume different values on different invariant subsections of an energy surface. One would hope - looking at the pleasant properties of uniform distributions on an E-surface - that this complication does not occur if H is not separable. But even in this case, when no further analytical constant of motion besides energy exists, the motion of a particle is not necessarily ergodic.

More recent works by Kolmogorov (1954), Arnold (1961), Moser (1962), and computer calculations by Hénon and Heiles (1964) and others have shown that even in general situations - provided ε not too large - an energy surface will be separated by invariant tori possessing Lebesgue measure greater zero. Besides such ordered motion on invariant tori other trajectories exist which wander all over the whole energy surface.

Summarizing, it can be stated that even for general functions $\lambda(r,z)$, distribution functions nonuniform on an energy surface exist, and one is kept to believe that such a distribution will result from a uniform distribution if some external parameter is changed adiabatically. At the same time, however, it appears to be impossible - with present knowledge - to incorporate our informations on the topological situation on an energy surface in the explicit construction of a distribution function other than uniform on an energy surface.

Special cases where approximate additional constants of motion (rsp. adiabatic invariants) exist, are treated in C IV.

II. An Adiabatic Invariant and Invariant Distribution Function

Consider a uniform population of the surface $H = E$. Through an adiabatic change of the Hamiltonian $H \rightarrow \tilde{H}$, this uniform population shall be transformed into another on $\tilde{H} = \tilde{E}$. The new energy $\tilde{E}$ can be obtained by applying Liouvilles theorem, which states that phase space volume remains constant for a Hamiltonian flow. Hence

$$(19)\quad I(E,\tau) \equiv \int_{H(p_r,p_z,r,z,\tau)\leqq E} dp_r\, dp_z\, dr\, dz$$

shall be used as adiabatic invariant for a Hamiltonian $H = \frac{p_r^2+p_z^2}{2m} + V(r,z,\tau)$, where τ introduces a slow time dependence. Favoured by the given number of dimensions, integration over momentum space can be easily done ($\rho^2 \equiv p_r^2 + p_z^2$):

$$(20)\quad I(E,\tau) = \pi \int dr\, dz \int_0^{2m(E-V)} d\rho^2 = 2\pi m \int_{E-V\geqq 0} (E-V)\, dr\, dz$$

With the inverse of $I(E,\tau)$ an invariant distribution function $F^\circ(I)\, dI$ is obtained from $f^\circ(H,\tau)\, dp_r\, dp_z\, dr\, dz$

$$(21)\quad F^\circ(I)\, dI \equiv \int_{E(I,\tau)\leqq H \leqq E(I,\tau)+\frac{\partial E}{\partial I} dI} f^\circ(H,\tau)\, dp_r\, dp_z\, dr\, dz = f^\circ(H,\tau)\, dI$$

Hence $F^\circ(I) = f^\circ(H(I,\tau),\tau)$. $F^\circ(I)$ may be prescribed as initial condition. The physical density (besides integration over p_θ) is evaluated as:

$$(22)\quad n(r,z)\, dr\, dz = \int f^\circ(H,\tau)\, dp_r\, dp_z = 2\pi m \int_0^\infty F^\circ(I(H,\tau))\, dT$$

with $T \equiv \frac{p_r^2+p_z^2}{2m}$; total particle numbers are $N_e = \iint dp_\theta\, g_e^\circ(p_\theta) F_{e\perp}^\circ(I)\, dI$ and $N_i = \int F_i^\circ(I)\, dI$

III. Basic Integro-Differential-Equations

With above defined invariant distributions for electrons $(F_{e\perp}^\circ)$ and ions (F_i°) selfconsistency is established by solving the following coupled nonlinear integro-differential equations for the self-potentials A_0^{self}, Φ_0^{self}, applied to the approximation B III:

$$(23)\quad \overset{*}{L}{}^{self} A_0 \equiv \left(\frac{\partial}{\partial r}\frac{1}{r}\frac{\partial}{\partial r}r + \frac{\partial^2}{\partial z^2}\right)A_0^{self} = -\frac{4\pi e m_0 \gamma_0}{c\,r}\int dP_\theta q_e^0(P_\theta) v_{\theta_0} \int F_{e\perp}^0\left(I\left(T+\frac{e}{c}v_{\theta_0}A_0^{self} - e\phi_0^{self} + V_{0e}^{ext}, \tau\right)\right)dT$$

$$(24)\quad L\phi_0^{self} \equiv \left(\frac{1}{r}\frac{\partial}{\partial r}r\frac{\partial}{\partial r} + \frac{\partial^2}{\partial z^2}\right)\phi_0^{self} = \frac{4\pi e m_0 \gamma_0}{r}\left(\int dP_\theta q_e^0(P_\theta)\int F_{e\perp}^0\left(I\left(T+\frac{e}{c}v_{\theta_0}A_0^{self} - e\phi_0^{self} + V_{0e}^{ext}, \tau\right)\right)dT - \right.$$
$$\left. - r\int F_i^0\left(I\left(T+e\phi_0^{self} + V_{0i}^{ext}, \tau\right)\right)dT\right)$$

For given functions $F_{e\perp}^0(I)$, $q_e^0(P_\theta)$, $F_i^0(I)$, external potentials $V_{e,i}^{ext}$ and boundary conditions the equations (23, 24) together with (20) have to be solved by an appropriate iteration scheme, to give a fixpoint for the desired physical solution - a sometimes difficult task, which will be discussed in section D.

IV. Approximations for the Transverse Distribution Function of Electrons

In two special cases the existence of an additional - approximate - adiabatic invariant should be considered for the construction of electron distribution functions.

1. Nearly decoupled motion

If the uncoupled forces acting on electrons in either direction r, z are large compared to the coupling force - nonlinear resonances being absent - individual (decoupled) adiabatic invariants I_r, I_z may be considered. An invariant distribution function is then $F_{e\perp}^0\left(I_r(H_r,\tau), I_z(H_z,\tau)\right)$ with $H_r = \frac{p_r^2}{2m} + V(r,0,\tau)$, $H_z = \frac{p_z^2}{2m} + V(0,z,\tau)$ and

$$(25)\quad I_r(E_r,\tau) = \int\limits_{H_r \leqq E_r} dp_r\, dr \quad , \quad I_z(E_z,\tau) = \int\limits_{H_z \leqq E_z} dp_z\, dz$$

2. Scaled oscillation frequencies

If the coupling force is not weak, but the radial and axial oscillation frequencies obey a scaling law $\frac{\nu_r}{\nu_z} \gg 1$ another approximation is possible. In this case changes in z are slow compared to changes in r and the former may be considered adiabatic, which introduces an additional adiabatic invariant.

This approximation appears to be realistic for electrons in an electron ring with moderate space charge densities and small field index n, since the term $\sim (1-n)\delta_r^2$ in the Hamiltonian (17) renders the r-motion rapid as compared with the z-motion. In standard form (17) is written as

$$H = \frac{p_r^2 + p_z^2}{2} + V(r,z,\tau)$$

Using the scaling $\nu_r \gg \nu_z$, the r-motion is described by

$$\hat{H} = \frac{p_r^2}{2} + V(r,z,\tau)$$

with an adiabatic invariant

$$\hat{I}(\hat{H},z,\tau) = \int dp_r\, dr \qquad (26)$$

Let a solution of the z-equation of motion $\ddot{z} = -\frac{\partial V(r,z,\tau)}{\partial z}$ be written as $z = Z(t) + \zeta(t)$,

where $\zeta(t)$ is the oscillating part caused by the coupling with the r-motion. For simplicity V is assumed symmetric in r and one then expands V around the zero order motion $Z(t)$

$$\ddot{Z}(t) + \ddot{\zeta}(t) = -\frac{\partial V}{\partial z} = -\frac{\partial}{\partial Z}\left\{V(0,Z,\tau) + \frac{\partial V}{\partial Z}\zeta + \frac{\partial V}{\partial r} r + \frac{\partial^2 V}{\partial r^2}\frac{r^2}{2} + \dots\right\}$$

Averaging over the rapid time dependence yields without higher orders

$$\ddot{Z} = -\frac{\partial}{\partial Z}\left\{V(0,Z,\tau) + \frac{\langle r^2\rangle}{2}\frac{\partial^2 V}{\partial r^2}\right\} \qquad (27)$$

With $\langle r^2\rangle = u(\hat{I},Z,\tau)$ an effective potential is found according to $\frac{\partial V_{eff}}{\partial Z} = \frac{\partial V}{\partial z} + u(\hat{I},Z,\tau)\frac{\partial^2 V}{\partial r^2}\Big|_{r=0}$

and the Z-motion is governed by

$$\tilde{H} = \frac{P_Z^2}{2} + V_{eff}(0,Z,\tau,\hat{I}) \qquad (28)$$

The second adiabatic invariant is then

(26') $\tilde{I}\left(\tilde{H}, z, \hat{I}\right)$

and invariant distribution functions are

(29) $f_{e\perp}\left(\hat{H}, \tilde{H}, z, z\right) \equiv F^{\circ}_{e\perp}\left(\hat{I}, \tilde{I}\right)$

The class of distributions (29) is apparently larger than the class of distributions $F^{\circ}_{e\perp}\left(I(H,z)\right)$ (B.II).

For either approximation 1) or 2) densities have to be calculated by separate integration over p_r, p_z in contrast to the distribution $F^{\circ}_{e\perp}(I)$, which allowed for reduction to a one-dimensional integration over $dT \equiv d\left(\frac{p_r^2+p_z^2}{2m}\right)$

V. The Ion Distribution Function

For strongly nonuniform electron density the potential acting on ions introduces sufficient coupling in r,z as to prohibit approximation IV.1) for ions; approximation IV.2) also fails because the radial and axial ion oscillation frequencies only differ by little. This calls for ergodic behaviour of trajectories and the use of distribution functions $F_i(I)$, the detailed form of which will be derived in this section.

The most convenient way of introducing ions to an ER is by rest-gas-ionization. Ions are born with zero kinetic energy in the potential t rough built up by the electric space charge. The ionization probability is proportional to electron density. Thus ion density is expected to be more peaked in the center of the ring than electron density.

Within the framework of the present model, a selfconsistent building up of $F^{\circ}_i(I)$ is obtained through the following equation, assuming an ionization rate α_i constant in time, and ionization slow enough to sustain adiabaticity.

$$(30)\quad \frac{\partial \overset{\circ}{F}_i(I,t)\,dI}{\partial t} = \alpha_i \int_{E(I,t) \le e\phi_0^s(r,z,t) \le E(I,t)+\frac{\partial E}{\partial I}dI} \overset{\circ}{n}_e(r,z,t)\,dr\,dz$$

with the Hamiltonian $H_i^\circ = \frac{p_r^2+p_z^2}{2m_i} + e\phi_0^s$ ($V_{0_i}^{ext} \equiv 0$ during ionization). The integral can be transformed into a line integral along equipotential lines of the potential $V = e\phi_0^s$ with a line-element $d\sigma$:

$$\frac{\partial \overset{\circ}{F}_i}{\partial t}\,dI = \alpha_i\, dV \int \overset{\circ}{n}_e(r,z,t)\,\frac{\partial(r,z)}{\partial(V,\sigma)}\,d\sigma$$

$$(31)\quad = \alpha_i \frac{\partial E}{\partial I}\,dI \int_{V=E} \overset{\circ}{n}_e(r,z,t)\,\frac{\partial(r,z)}{\partial(V,\sigma)}\,d\sigma$$

The functional determinant for the transformation into curvilinear coordinates V,σ is derived as

$$\frac{\partial(r,z)}{\partial(V,\sigma)} = \left(|\nabla V|\right)^{-1}$$

then

$$(32)\quad \frac{\partial F_i(I,t)}{\partial t} = \alpha_i \frac{\partial E(I,t)}{\partial I} \int_{V=E(I,t)} \frac{\overset{\circ}{n}_e(r,z,t)}{|\nabla V|}\,d\sigma$$

Since $\overset{\circ}{n}_e$ and V are affected by the ion space charge, above equation has to be discretized in time and at each step solved simultaneously with equations (23,24).

$$(32')\quad \Delta F_i(I,t) = \Delta t\,\frac{\partial F_i(I,t)}{\partial t}$$

VI. Polarization and Particle Loss During Acceleration

When an accelerating field is applied in z-direction (B_r or E_z field), opposite forces act on ions and electrons, which tend to polarize the ring in z-direction. For sufficiently high acceleration, particles start to evaporate from the ring as a result of the decrease in axial focusing. Thus ions will be lost; also electrons, if besides ion space charge there is no other mechanism present to focus electrons axially (like a "Squirrel Cage").

Equilibrium during acceleration is conveniently studied in an accelerated system of reference, in which the electron-ion ring as a whole is forcefree.

Such a system is known as Möller-system (Möller, 1943); for small acceleration and not too large axial beam dimensions it permits an approximation by a system in which a uniform gravitation force acts which is equal to the acceleration in the laboratory frame.

Consider for example magnetic acceleration in an acceleration column where a small B_r is present. The following additional forces appear in the Hamiltonian:

$$(33)\quad \tilde{H}^{\circ}_{e_\perp} = H^{\circ}_{e_\perp} + \left(e\frac{V_{z_0}}{c}B_r - m_0\gamma_0 b\right)z = H^{\circ}_{e_\perp} + \tau' z$$

$$(34)\quad \tilde{H}^{\circ}_{i} = H^{\circ}_{i} + \left(-m_i b\right)z = H^{\circ}_{i} - \tau z$$

where it is assumed that the axial velocity is nonrelativistic. Force-balance yields:

$$\left(e\frac{V_{z_0}}{c}B_r - m_0\gamma_0 b\right)N_e + (-m_i b)N_i = 0 \quad\rightarrow\quad \tau' = f\tau$$

$$(35)\quad b = \frac{e\frac{V_{z_0}}{c}B_r}{m_i f + m_0\gamma_0} = \frac{\tau}{m_i}$$

$H^{\circ}_{e_\perp}$, H°_{i} contain selffield-potentials which depend on τ implicitly. The additional term $\sim \tau z$ leads to a pass in the potential at some $V = E_{pass}$ (to be determined selfconsistently), which causes particle overflow if $E > E_{pass}$. Evaporation through such a pass starts if τ is larger than some $\tau_{threshold}$.

Clearly, variable particle numbers during acceleration must be expected to introduce new stability properties of any iteration scheme to solve (23,24).

D. Iteration Scheme for a Numerical Code

The set of equations (23), (24), (30) and (20) or (25) or (26), (26') prescribing the adiabatic processes of compression, ion loading and acceleration has to be solved by iteration. For given parameters N_e, γ, f, τ (acceleration) and functions B_0^{ext}, $F_{e\perp}^0$ (initial condition), a selfconsistent solution or fix-point of above equations is supposed to exist for physical reasons. Since ion-loading and acceleration including particle loss are slowly time dependent and irreversible processes, a fix-point depends on time as a continuous parameter.

A discretization with respect to this slow time is required therefore. At each step selfconsistency has to be established by iteration.

Convergence of an iteration scheme - assumed a fix-point exists - depends critically on the mathematical properties of the operator defining the fix-point problem (i.e. its eigenvalue spectrum). These properties may be described in terms of some physical quantities: number of particles to be confined, attractive or repulsive selfforces, several particle species, dependence of the number of confined particles on selffields or not, external potentials, boundary conditions.

As far as the author knows, no criteria are available dealing with existence or uniqueness of a fix-point of an appropriate iteration scheme for the present coupled equations problem.

The simplest "direct" iteration was attempted in the numerical code. In most of the cases it was convergent after few ($\lesssim 5$) iteration cycles. When iteration failed a relaxation was introduced which connected subsequent iteratives according to the following law:

$$\psi^{(n+1)} \equiv (1-\alpha)\psi^{(n)} + \alpha\psi^{(n+1/2)} \qquad (0 < \alpha \leq 1)$$

$\psi^{(n+1/2)}$ follows from $\psi^{(n)}$ through the scheme of equations; $\alpha = 1$ yields "direct" iteration, $\alpha \to 0$ decelerates the iteration velocity to zero. This "first order relaxation" is appropriate if the "direct" iteratives oscillate about some solution, whereas monotonically diverging "direct" iteratives require a "second order relaxation" : $\psi^{(n+1)} \equiv (1-\alpha)\,\psi^{(n)} + 2\alpha\,\psi^{(n+1/3)} - \alpha\,\psi^{(n+2/3)}$ (see B. Marder, H. Weitzner (1969)).

In the present case it was believed that the "direct" and "first order relaxation" methods were sufficient to numerically obtain a fix-point solution whenever there exists one in the physical sense. Hence divergence of <u>both</u> methods was used as criterium for nonexistence of an equilibrium solution. This is important to define a maximum admissible acceleration of rings (holding power).

The full scheme has the following structure:

subroutine EQUIL: calculates by iteration the potentials A_0^{self}, ϕ_0^{self} selfconsistent with given invariant distributions $F_{e\perp}^{0}$, F_i^{0} and external potentials V_{0e}^{ext}, V_{0i}^{ext} in toroidal geometry with appropriate boundary conditions.

subroutine IONIZ: solves equation (32) for differential ion production with given ϕ_0^{self}, n_e^0, α_i, Δt.

subroutine ADINV: is applied in EQUIL, IONIZ and calculates adiabatic invariants $I(E,t)$.

subroutine DENSI: is applied in EQUIL and calculates the density according to the right sides of equations (23), (24).

subroutines POISTR, EQU: are applied in EQUIL and solve the Poisson and vector potential equations for given densities and boundaries.

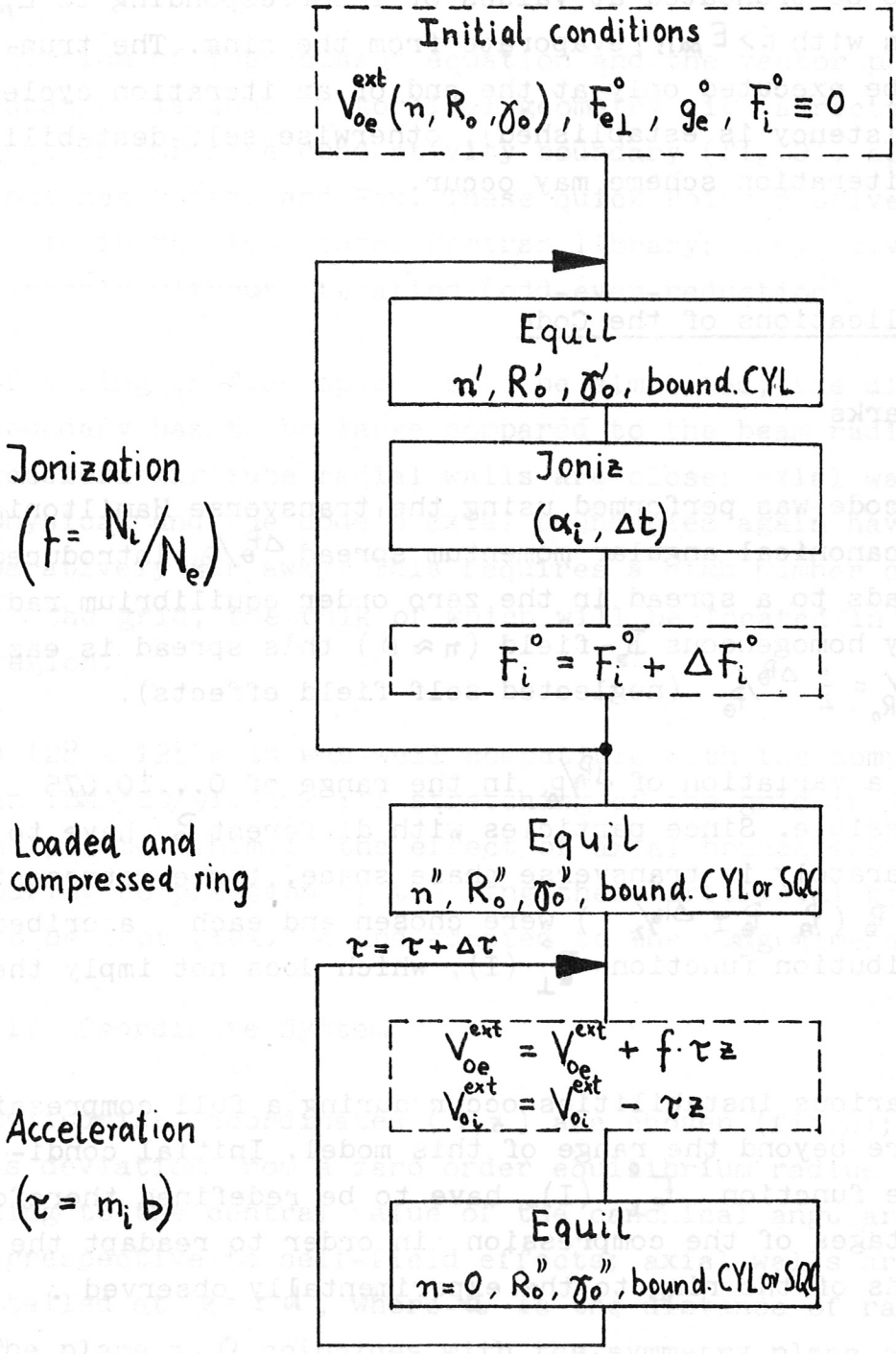
Initial conditions
$V_{oe}^{ext}(n, R_o, \gamma_o)$, $F_{e\perp}^{\circ}$, g_e°, $F_i^{\circ} \equiv 0$
Equil
n', R_o', γ_o', bound. CYL
Joniz
$(\alpha_i, \Delta t)$
$F_i^{\circ} = F_i^{\circ} + \Delta F_i^{\circ}$
Ionization
$(f = N_i/N_e)$
Equil
n'', R_o'', γ_o'', bound. CYL or SQC
Loaded and compressed ring
$\tau = \tau + \Delta\tau$
$V_{oe}^{ext} = V_{oe}^{ext} + f \cdot \tau z$
$V_{oi}^{ext} = V_{oi}^{ext} - \tau z$
Acceleration
$(\tau = m_i b)$
Equil
$n = 0, R_o'', \gamma_o''$, bound. CYL or SQC

If a pass occurs in the potential, the invariant distributions $F_{e\perp}^{o}$, F_{i}^{o} have to be truncated at values of I corresponding to E_{pass} since particles with $E > E_{pass}$ evaporate from the ring. The truncation should be executed only at the end of an iteration cycle (when selfconsistency is established), otherwise self-destabilization of the iteration scheme may occur.

E. Special Applications of the Code

I. General Remarks

The numerical code was performed using the transverse Hamiltonian of B.III. The canonical angular momentum spread $\Delta P_\Theta / P_\Theta$ introduced by $q_e^{o}(P_\Theta)$ leads to a spread in the zero order equilibrium radius R_o. For nearly homogeneous B_z-field ($n \approx 0$) this spread is easily derived as $\Delta R_o / R_o = \frac{1}{2} \Delta P_\Theta / P_\Theta$ (neglected self-field effects).

In experiments a variation of $\Delta P_\Theta / P_\Theta$ in the range of $0 \ldots \pm 0.075$ seems to be possible. Since particles with different P_Θ have to be treated separately in transverse phase space, three representative values of P_Θ (P_{Θ_o}, $P_{\Theta_o} \pm \Delta P_\Theta / 2$) were chosen and each ascribed the same distribution function $F_{e\perp}^{o}(I)$, which does not imply the same $f_{e\perp}^{o}(H,t)$

As is known, various instabilities occur during a full compression cycle, which are beyond the range of this model. Initial conditions, i.e. the function $F_{e\perp}^{o}(I)$, have to be redefined therefore at different stages of the compression in order to readapt the small dimensions of the ring to the experimentally observed .

Since a main effect of instabilities is an increase of the effective phase space, this redefinition is carried through by stretching the function $F_{e\perp}^{o}(I)$ to a larger range of I.

II. Boundary Conditions and Poisson Solver

Solution of the Poisson equation and the vector potential equation is done in toroidal geometry with a rectangular cross section infinite conductivity boundary (fig.2), applying subroutines Poistr and Equ. These quick Poisson solvers are available in the Institutes Fortran library; they solve the equations directly without iteration (odd-even-reduction).

If a ring in free space is to be simulated, the distance beam-boundary has to be large compared to the beam radius. In the accelerating tube radial walls are close; axial walls are unphysical and the code's axial boundaries again have to be comparatively far away. This requires a high number of mesh points on the grid, the bulk of which will be located in the vacuum region.

A 128 x 128 grid was well compatible with the computer memory - an IBM 360/91. A 2 : 1 stretching of the grid in axial direction helped to minimize the effect of axial boundaries on selffields. During compression of the ring these artificial boundaries have to be kept flexible and adapted to the ring dimensions.

III. Coordinate System

Cylindrical coordinates (r, z) are chosen (fig.2); r is defined as deviation from a zero order equilibrium radius R_0 corresponding to the central value of the canonical angular momentum P_{θ_0}, irrespective to self-field effects; axial walls are thought installed at $z = \pm d$, where d is the distance of radial walls. The plane $z = 0$ coincides with the symmetry plane of the magnetic mirror. For acceleration a system of reference is chosen where the ring as a whole is force-free.

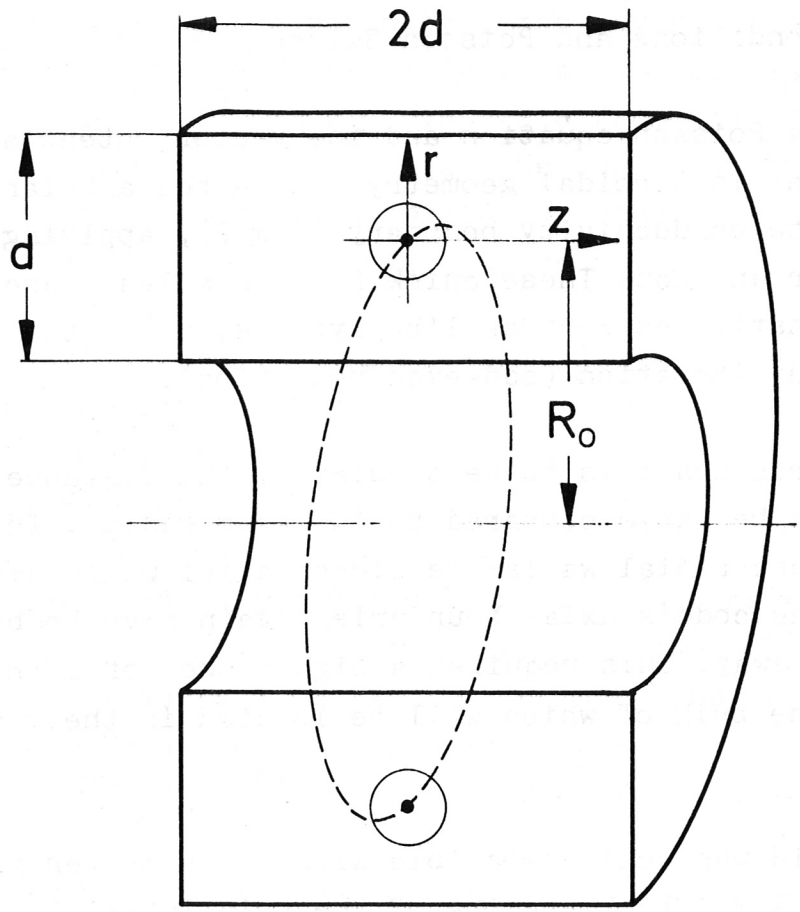

fig.2 Geometry

IV. Two Alternative Versions

To apply the considerations of C II and C IV, two versions were performed which differ in the electron distribution function:

Version I

Distribution functions $F^{o}_{e\perp}(I(H,t))$, i.e. distributions uniform on energy surfaces $H(p_r, p_z, r, z, t) = E$ are used according to C II. The resulting equilibria have the advantage to be exactly selfconsistent.

Version II

Distribution functions $F^{\circ}_{e\perp}\left(I_r(H_r,t),\ I_z(H_z,t)\right)$ are used according to C IV 1. These distributions are not exactly selfconsistent because they are based on decoupled Hamiltonians $H_r(p_r, r, t)$ and $H_z(p_z, z, t)$, where the coupling in the selffield potentials was omitted.

V. Electron Distribution Function

1. For Version I the invariant distribution function was chosen as $F^{\circ}_{e\perp}(I) \sim \exp\left(-(I/4I_{max})^{1/2}\right)\cdot\Theta(I-I_{max})$ with Θ the step-function. Since $I \sim E^2$ for purely quadratic potentials, this corresponds to a truncated Gauss-distribution $\exp\left(-E/2E_{max}\right)$ at the initial stage (uncompressed ring) when nonlinear self-fields are negligeable. I_{max} is chosen such as to obtain the small dimensions of the uncompressed ring, which for the Garching ERA experiment are typically of the order of $\bar{a} \approx \bar{b} \approx 0.5$ cm at $R_0 = 15$ cm, $\sigma_0 = 3.8$, $n = 0.5$. To fit with the experimental data the effective phase space volume had to be increased roughly by a factor of 7 until the end of the compression ($I_{max} \rightarrow 4 \cdot I_{max}$), thus taking into account the (nonadiabatic) work of instabilities.

A momentum spread $\Delta p_0/p_0 = \pm 0.075$ was introduced to have the radial beam dimension ($\bar{b}$) sufficiently large and close to the experimentally observed after compression ($\bar{b} \approx \bar{a}$).

2. For Version II a distribution $F^{\circ}_{e\perp}(I_r, I_z) \sim \exp\left(-\frac{I_r/\mu + I_z}{I_{max}}\right)\cdot$ $\Theta\left(I_r/\mu + I_z - I_{max}\right)$ was used, where the additional free parameter μ allowed an independent choice of occupied radial and axial phase space volumes. Thus a reasonably large radial ring dimension could be achieved without momentum spread, which was put zero in this version. Since $I_r \sim \varepsilon_r$ and $I_z \sim \varepsilon_z$ for quadratic potentials, this $F^{\circ}_{e\perp}$ represents again a truncated Gauss-distribution $\sim$ $\exp\left(-\frac{\varepsilon_r+\varepsilon_z}{\varepsilon_{max}}\right)$ at the initial stage (uncompressed ring).

VI. Normalization of Physical Quantities.

The following units were used in the code:

energy: $\langle E \rangle \equiv m_0 \gamma_0 V_{\Theta 0}^2 / R_0^2 \left(\rho_0/2\right)^2$, transverse energy before compression (field index $n = 0.5$) corresponding to a ring with small radius ρ_0, neglecting selffields.

length: $\langle l \rangle \equiv d$ initial radial distance of walls.

mass: $\langle m \rangle \equiv m_0 \gamma_0$ electron mass before compression

charge: $\langle e \rangle \equiv e$ elementary charge

particle number: $\langle N \rangle = N_e$ initial total number of electrons

VII. Ion Loading

Ions were "added" to the electron ring at the end of compression and at field index sufficiently different from zero to guarantee ring integrity. In one case only, ions were added earlier to study the influence hereof on the ion distribution function.

VIII. Squirrel Cage Simulation

A squirrel cage consists of a cylinder which is transparent to the magnetic field but not to the electric field of the ring (see G.V. Dolbilov et al. (1969) and I. Hofmann (1973)). Positive image charges on this cylinder thus yield an interesting focussing effect on axial betatron oscillations. In this code the outer cylinder was alternatively made a squirrel cage by shifting the (infinite conductivity) magnetic boundary to three times a distance from the ring than the electric boundary. Thus magnetic images only give a negligeable contribution ($\approx 1/3^2$ times the effect of electric images but opposite to it) to the fields inside the electron ring, which gives the desired magnetic transparency. The strength of the squirrel cage is characterized by $p_{sqc} \equiv \frac{R_0}{R_{sqc}}$ (R_{sqc} squirrel cage radius).

IX. Results

The subsequently prescribed computer runs were performed for rings with data that are representative for the Garching ERA experiment:

Number of electrons: $N_e = 5 \cdot 10^{12}$

Pre-compression data:

Equilibrium radius: $R_0 = 15$ cm (no selffield effects)

Field-index: $n = 0.5$

Relativistic mass factor: $\gamma_0 = 3.8$

Radius of small cross section: $\rho_0 = 0.5$ cm

Post-compression data (before ion loading, except example 5)

$R_0 = 2.3$ cm

$\gamma_0 = 27.2$

$n = 0.021$

Version I: estimated increase of occupied (p_r, p_z, r, z)-phase space by a factor 7

Version II: estimated increase of 2 -dim. occupied phase space (p_r, r) by a factor 54 and (p_z, z) by a factor 9 .

Ion-loading (protons):

Fractional ionization: $f = \frac{N_i}{N_e}$, $0 < f \leq 0.05$

The post-compression and ion loading states are calculated with boundary CYL: two infinitely conducting cylinders at $r = R_0 \pm 1.25$, closed axially at $z = \pm 2.5$.

Accelerating tube (force on ions: $\kappa = m_i b$ for magnetic acceleration; $R_0 = 2.3$ cm, $\gamma_0 = 27.2$, $n = 0$):

a) boundary CYL; or alternatively:

b) boundary SQC; squirrel cage at $r = R_0/p_{sqc}$ $(0.60 \leq p_{sqc} \leq 0.8)$, infinitely conducting cylinder at $r = R_0 - 1.25$, closed axially at $z = \pm 2.5$

Momentum spread (only for Version I):

Three subrings at $r = R_0$, $R_0 \pm \Delta R_0$ with $\Delta R_0/R_0 = \frac{1}{2}\Delta p_0/p_0 = 0.0375$ (in this case above R_0, γ_0 are only average values).

For the following rungs equilibrium functions are plotted and characteristic properties listed in table 1.

Example ①

Version I; f = 0.025 at post-compression; acceleration in boundary SQC; P_{sqc} = 0.7; fig. 14, 15

Example ②

Version II; f = 0.05 at post-compression; acceleration in boundary CYL; fig. 3, 4, 7, 9, 10, 13

Example ③

same with f = 0.025; fig. 13, 15

Example ④

same with f = 0.0175; fig. 5, 7, 13

Example ⑤

Version II; f = 0.05 during compression at R_o = 5 cm, γ = 13, n = 0.01; acceleration in boundary CYL;

Example ⑥

Version II; f = 0.025 at post-compression, acceleration in boundary SQC; P_{sqc} = 0.8; fig. 14

Example ⑦

same with f = 0.001; fig. 14

Example ⑧

same with f = 0.025; P_{sqc} = 0.7; fig. 3, 6, 8, 9, 10, 14, 15

Example ⑨

same with f = 0.001; fig. 3, 6, 8, 9, 14, 15

Example (10)

same with $f = 0.025$; $\rho_{sqc} = 0.65$; fig. 14

Example (11)

same with $f = 0.001$; fig. 14

Example (12)

same with $f = 0.05$; $\rho_{sqc} = 0.6$; fig.13

Example (13)

same with $f = 0.025$; fig.9, 10, 13

Example (14)

same with $f = 0.025$; $\rho_{sqc} = 0.7$; electron radial and axial occupied phase space increased by a factor 4; fig.14

Example (15)

post-compression (before ion loading) in boundary CYL*: two cylinders at $r = R_0 \pm 2.21$, closed axially at $z = \pm 4.41$; same electron phase space as in examples (6) - (13)

Example (16)

same as (15) with electron phase space reduced by a factor 4

Table 1 contains ring data for unaccelerated rings, which are significant for the holding power:
$2\bar{a}$ and $2\bar{b}$ axial and radial electron ring width at half maximum density; ΔR_0, ΔR_i shift of electron ring equilibrium radius and ion ring c.o.m. with respect to vacuum R_0; $e\mathcal{E}_{z\,peak}$, $e\mathcal{E}_{z\,edge\,ions}$ peak electric field and electric field at the edge of ion subring as produced by the electron space charge; $\Delta\nu_z^2$ self-field contribution to squared axial tune of electrons (included toroidal and image effects); ΔN_e fraction of electrons lost due to insufficient axial focussing.

	$\bar{a}$ [cm]	$\bar{b}$ [cm]	ΔR_o [cm]	ΔR_i [cm]	$eE_{z\,peak}$ [MeV/m]	$eE_{z\,edge\,ions}$ [MeV/m]	$\Delta \nu_z^2$	ΔN_e [%]
example ① post-compression (before ion loading)	.27	.12	.002	-	29	-	-.0074	0
$f = .025$ $P_{SQC} = .7$ in acc.tube SQC	.20	.12	.011	-.008	28	25		0
example ②-④, ⑥-⑬ post-compression (before ion loading)	.32	.29	.0023	-	24	-	-.0067	0
example ② $f = .05$ in acc.tube CYL	.23	.30	.0008	-.035	22	22	-.0069	3%
example ③ same with $f = .025$	.25	.30	.0009	-.039	15	15	-.0047	34%
example ④ same with $f = .0175$	.23	.31	.0008	-.041	12	9	-.0036	49%
example ⑤ during compression (before ion loading)	.85	1.25	.0008	-	4	-	-.0038	0
$f = .025$ in acc.tube CYL	.27	.31	.0009	-.046	13	8.5	-.0040	38%
example ⑥ $f = .025$ $P_{SQC} = .8$ in acc.tube SQC	.25	.29	.030	-.065	25	23	.026	0
example ⑦ same with $f = .001$	.29	.29	.026	-.073	24	22	.025	0
example ⑧ $f = .025$ $P_{SQC} = .7$ in acc.tube SQC	.30	.29	.013	-.037	21	21	.0010	0
example ⑨ same with $f = .001$	.50	.29	.013	-.044	17	17	.0022	0
example ⑩ $f = .025$ $P_{SQC} = .65$ in acc.tube SQC	.31	.29	.009	-.030	19	19	-.0018	0
example ⑪ same with $f = .001$	.70	.29	.009	-.039	13	13	.0002	0
example ⑫ $f = .05$ $P_{SQC} = .6$ in acc.tube SQC	.20	.23	.008	-.035	29	27	.0053	0
example ⑬ same with $f = .025$	.30	.31	.008	-.043	25	24	-.0037	0
example ⑭ post-compression (before ion-loading)	.62	.57	.0016	-	11	-	-.0037	0
$f = .025$ $P_{SQC} = .7$ in acc.tube SQC	.82	.57	.013	-.11	8	7.5	.0041	0
example ⑮ post-compression boundary CYL*	.34	.29	.010	-	22	-	-.0096	0
example ⑯ post-compression boundary CYL*	.19	.15	.01	-	47	-	-.013	0

Table 1. Characteristic ring data for unloaded electron rings and loaded rings at rest in accelerating tube $(n=0)$

X. Discussion of Results

1. Existence of strictly self-consistent equilibrium solutions with accelerating forces was shown through runs with Version I (ex. (1)). Since oscillation energies of electrons in radial and axial directions are equal in this version, the ring cross sections deviate strongly from circular, i.e. $\bar{b}$ is apparently smaller than $\bar{a}$. In particular, the radial dimension $\bar{b}$ is governed by the momentum spread in this case. The equilibria belonging to increasing accelerating forces cannot be claimed to result from each other dynamically since the adiabatic invariant connecting them is probably inappropriate. Parameter studies were carried out with Version II which, owing to the decoupled electron motion is supposed to well approximate electron's dynamical behaviour. It also allows for realistic electron density cross sections. The main results from ex. (2) - (16) are:

2. Inhomogeneous electron and ion densities.

Figures 4-6 show that the ion density is more peaked than the electron density with half-widths that are smaller by at least a factor 2. The shape of the axial electron density profiles depends on the boundary (CYL or SQC), whereas the radial profiles are nearly independent hereof, as was expected. The ion density is quite insensitive to the shape of the electron density, the ion ring cross section nearly circular. Of some interest is the study of the difference in holding power which occurs when ions are added to a ring which is not yet completely compressed, i.e. has still larger $\bar{a}, \bar{b}$ (by a factor $\gtrsim 3$ in ex. (5)). After complete compression of the loaded ring an equilibrium results which has worse properties than in ex. (3): the holding field $e\mathcal{E}_{z\,\text{peak}}$ ($e\mathcal{E}_{z\,\text{edge ions}}$) is only 13 (8.5) instead of 15 (15) MeV/m in ex. (3); this is due to the fact that the phase space filled up by ions is now by a factor 2.3 larger, which increases the small diameter of the ion ring by a factor 1.25.

3. Anharmonic betatron oscillations.

If ion focussing is dominant, axial electron oscillations are strongly anharmonic due to the nonuniform ion space charge (fig.11, ex. ②, the oscillation frequencies ν_z are calculated using the formula $\nu_z^{-1} = 2\pi \frac{\partial I_z}{\partial E_z}$). With nearly pure squirrel cage focussing (ex. ⑧) the tune ν_z is practically independent of the oscillation energy or amplitude, since image fields vary linearly within the ring dimensions.

4. Toroidal effects.

In relativistic electron rings an axial defocussing force occurs in addition to the $1/\gamma^3$-repulsion of straight relativistic beams. This toroidal effect is usually much stronger than the $1/\gamma^2$ - effect and poses severe limits to the number of electrons confinable in the ring without external focussing. An $f \gtrsim 0.05$ was necessary in ex. ② to make ion focussing efficient enough not to lose electrons. Fig.7, ex. ② shows the limiting case: smaller f leads to loss of "hotter" electrons like in ex. ④ ($f = 0.0175$), where only half of the originally present eletrons are confined and the oscillation energy is substantially reduced. Ion confinement is not changed by this variation of f, because ions are always attracted by the strong electron space charge.

We remind that in ex. ②, ④ (also ③, see table 1) the same initial electron ring was used before ion loading. The confinement threshold $f \approx 0.05$ can be reduced only by lowering the electron axial "temperature", which is not an easy task from the experimental point of view. The remaining remedy is an external focussing, for instance image focussing by a squirrel cage. A small amount of image focussing is already present in ex. ②-④ due to the relatively close perfectly conducting walls. Instead of the defocussing contribution $\Delta\nu_z^2 = -0.0067$ for ex. ②, even $\Delta\nu_z^2 = -0.0096$ was obtained in ex. ⑮, where the outer image cylinder had a radius of $r = 4.51$ cm and the inner image cylinder of $r = 0.09$ cm (table 1). Hence the above confinement threshold ($f \approx 0.05$) is still larger if these image cylinders are removed.

Finally toroidicity leads to a radial force and a force gradient. The radial force shifts the equilibrium radius to $R_o + \Delta R_o$ and the ion c.o.m. to $R_o + \Delta R_i$. Of course, the values listed in table 1 result from the common effect of toroidicity and image cylinders.

5. Squirrel cage focussing

Ex. (2) - (4) are compared with the results obtained when a squirrel cage is added to the system before $n \to 0$. Depending on the ratio of radii, P_{sqc}, the total self-field contribution to $\Delta\nu_z^2$ can be made positive, which guarants focussing independent of ions (ex. (6) - (13)).

We observe (ex. (11) that $P_{sqc} = 0.65$ is sufficient to have all electrons confined even for a small fractional ionization $f = 0.001$ (fig.8). In this case the self-field-$\Delta\nu_z^2$ is positive; it becomes slightly negative if f is increased to 0.025, because the axial compression of the ring due to ions makes the repulsive toroidal effects stronger. The same effect is observed in ex. (14), where a thicker ring (higher electron "temperature") shows a higher value of $\Delta\nu_z^2$ than in ex. (8), of course on the expense of the holding field $e\mathcal{E}_{z\,peak}$.

Correspondingly a thinner ring decreases $\Delta\nu_z^2$ as shown in ex. (16). As a rough estimate an increase (or decrease) of the small ring dimensions by a factor 2 gives a contribution $\Delta\nu_z^2 \approx 0.003$ (or -0.003).

Again we recall that in geometries where the additional inner cylinder is absent, the actual $\Delta\nu_z^2$ has to be reduced by an amount of the order of 0.001 - 0.002 (for our parameters), which may be compensated by a somewhat larger P_{sqc} (see I. Hofmann, 1973).

6. Holding power

When accelerating forces are applied to the electron-ion-ring a polarization occurs (fig.12) as a result of which the axial focussing of either particle species is reduced. In order to make cases with different ion loading and boundaries comparable with each other, the same initial ring (fully compressed, before ion loading) was chosen in all examples - except ex. (5), (14). The following subdivision is made, depending on the sign of $\Delta\nu_z^2$:

a) insufficient image focussing: the self-field contribution $\Delta\nu_z^2$ is negative and for low ion loading electron confinement is violated (ex. (2) - (4) and (12) - (13); table 1). In this case electrons are first lost from the accelerated system (fig.13, 15). Close to the maximum acceleration ions also evaporate from the ring and thus support rapid ring disintegration. As fig.13 shows (ex. (2) - (4)) the maximum admissible acceleration depends strongly on f. Nearly no acceleration is possible for $f = 0.0175$ (ex. (4)), which indicates the existence of a lower limit for f much larger than $1/f^2$.

An insufficient squirrel cage ($P_{sqc} = 0.6$) was looked at in ex. (12), (13). For $f = 0.025$ accelerated equilibria could be found in the vicinity of $m_i b = 4$ MeV/m, but not for lower $m_i b$. Failure of convergence of iteration in this case should be due to the form of the axial potential of electrons (fig.9, 10). In fig.10 two potential minima exist, which besides a solution with one ring allows for a second solution with two axially separated rings. Hence in this case the solutions of the basic integro-differential-equations may be expected to have a bifurcation point, in the vicinity of which iterative search of solutions often is a very intricate task.

b) dominant squirrel cage focussing: for $P_{sqc} = 0.65, 0.7, 0.8$ (ex. (6) - (11), (14)) electrons are focussed independently from ions. Electron loss occurs only after substantial reduction of the original number of ions N_{i_0} (ring disintegration, see fig.14).

The relative loss of ions N_i/N_{i0} is independent of f for the "good" squirrel cage $P_{sqc} = 0.8$, whereas it depends slightly on f for decreasing P_{sqc}.

Ex. (1) in fig.14 shows for comparison the ion loss for a run with Version I. N_i/N_{i0} decreases stronger than linearly (as in VersionII). This is due to the different adiabatic invariants used. To demonstrate the difference we compare them for parabolic potentials: $I \sim E^2/(\omega_x \cdot \omega_z)$ for Version I and $I_z \sim E_z/\omega_z$ for Version II. With acceleration ω_z is lower and we recognize that the adiabatic "cooling" of electrons goes like $E \sim \omega_z^{1/2}$ in Version I and $E_z \sim \omega_z$ in Version II, which means better confinement of ions in Version II.

Summarizing, squirrel cage focussing is desirable during acceleration. It should be as strong as to make the self-field contribution $\Delta\nu_z^2$ for electrons positive. In this case the holding power (maximum admissible acceleration) is nearly independent of f and reaches values of up to 80% of the peak electric field for a residue of ions.

Acknowledgement

The author is indebted to Prof. A. Schlüter and Dr. P. Merkel for valuable discussions on this subject. He particularly acknowledges the competent assistance of E. Springmann in the numerical part.

Bibliography

V.I. Arnold, in V.I. Arnold and A. Avez, Problèmes Ergodiques de la Mécanique Classique, Paris 1967

J.P. Boris, R. Lee, Computations on Relativistic Electron Beams and Rings, NRL Report 2284 (1971)

C. Bovet, Holding Field of a Nonuniformly Charged Electron Ring, LRL Berkeley Report ERAN 88 (1970)

R.C. Davidson, J.D. Lawson, Self-Consistent Vlasov Description of Relativistic Electron Ring Equilibria, University of Maryland Report 204P029 (1972)

R.C. Davidson, S.M. Mahajan, A Relativistic Electron Ring Equilibrium with Thermal Energy Spread, Part.Acc., 4, 53 (1972

G.V. Dolbilov et al., JINR-P9-4737, Dubna (1969)

A.A. Drozdovskii, On the Distribution Function of Ions Produced in an Electron Ring, Report ITEF-10, Moscow (1973)

M. Hénon, C. Heiles, Astron.Journ., 69, 73 (1964)

I. Hofmann, Focussing of an Electron Ring in the Presence of a Squirrel Cage and Conducting Cylinder, IPP-Report 0/16 (1973)

N.Y. Kazarinov, E.A. Perelshtein, Numerical Solution for the Stationary Problem of an Accelerated Self-Focussed Electron Ion Ring (transl.), Symposium on Collective Methods of Acceleration, Dubna (1972)

W.H. Kegel, Some Properties of Relativistic Plasma Rings, Plasma Physics, 12, 105 (1969)

A.N. Kolmogorov, in R. Abraham, Foundations of Mechanics, Appendix D, New York (1967)

L.J. Laslett, On the Focussing Effects Arising from the Self-fields of a Toroidal Beam, LRL Berkeley Report ERAN 30 (1969)

Concerning the Adiabatic Damping of Betatron Oscillations in an Electron Ring Compressor, ERAN 159 (1971)

Concerning the Electrostatic Field of Ions Loaded into a Uniform Electron Beam, ERA 19, Proceedings of Symposium on Electron Ring Accelerators (1968)

B. Marder, H. Weitzner, Plasma Physics, 12, 435 (1969)

P. Merkel, On the Holding Power of a Relativistic Electron Ring, IPP-Report 0/18 (1973)

D. Möhl, L.J. Laslett, A.M. Sessler, On the Performance Characteristics of Electron Ring Accelerators, Proceedings of the Symposium on Collective Methods of Acceleration, Dubna (1972)

C. Möller, On Homogeneous Gravitational Fields, Proceedings of the Danish Academy of Science, 2, No.19 (1943)

J. Moser, Nachr.Akad.Wiss.Gött., 1, 1 (1962)

W.A. Perkins, Criterion for Ion Focussing and Image Focussing during Extraction, LRL Berkeley Report ERAN 97 (1970)

S. Yoshikawa, Toroidal Equilibrium of a Relativistic Electron Ring, Princeton University Report MATT-816 (1972)

Figures

(Densities with maximum normalized to 1)

fig.3 Electron density profiles at post-compression (before ion loading; n = 0.021) for examples ② - ④, ⑥ - ⑬.

fig.4 Electron and ion (dashed) density profiles for example ② (CYL)

fig.5 Electron and ion (dashed) density profiles for example ④ (CYL)

fig.6 Electron and ion (dashed) density profiles for examples ⑧, ⑨ (SQC)

fig.7 Axial potentials for electrons and ions (dashed) in bound. CYL (②, ④)

fig.8 Axial potentials for electrons and ions (dashed) in bound. SQC (⑧, ⑨)

fig.9 Axial potential for electrons in bound. SQC (⑬)

fig.10 Axial potential for electrons in bound. SQC (⑬) with acceler. $m_i b$ = 4 MeV/m

fig.11 Electron axial oscillation frequency as function of oscillation energy for examples ② (CYL) and ⑧, ⑨ (SQC)

fig.12 Axial polarization as function of accelerating force for examples ② (CYL) and ⑧ (SQC); Δ = shift of electron and ion c.o.m.; $\bar{a}_o$ = half axial half-width of electron density at zero acceleration.

fig.13 Electrons in the ring in fractions of originally (before roll-out) present electrons as function of accelerating force for examples with insufficient (⑫, ⑬: P_{SQC} = 0.6; f = 0.05, 0.025) or no (②, ③, ④: bound. CYL; f = 0.05, 0.025, 0.0175) squirrel cage focussing. No loss of ions until ring disintegration (dotted appendices).

fig.14 Ions held by the ring (in fractions of originally present ions) as function of accelerating force for examples with dominant squirrel cage focussing. No loss of electons un-

til ring disintegration (dotted appendices). The hatched regions cover a range of f : $0.001 \leqq f \leqq 0.025$ (⑦, ⑨, ⑪ : $f = 0.001$; ⑥, ⑧, ⑩, ⑭ : $f = 0.025$).

fig.15 Density plots for electrons and ions in (r,z)-cross sections.

a) post-compression (before ion loading, $n = 0.021$);

b) loaded ring at $n = 0.005$ or $n = 0.002$ (①, ⑧, ⑨); accelerated rings.

For ex. ①, ⑧, ⑨ the ring is in a SQC at $n = 0.002$ and during acceleration.

The plots show lines of constant density $n_e(r,z)$ and $n_i(r,z)$ with uniform level difference Δn. The ion sub-ring is more compact than the electron ring and shifted to smaller radii. In ex. ① the electron density results from superposition of three rings with different P_θ and very small radial dimensions, which explains the spikes in the contours. The dotted horizontal line indicates the vacuum equilibrium orbit.

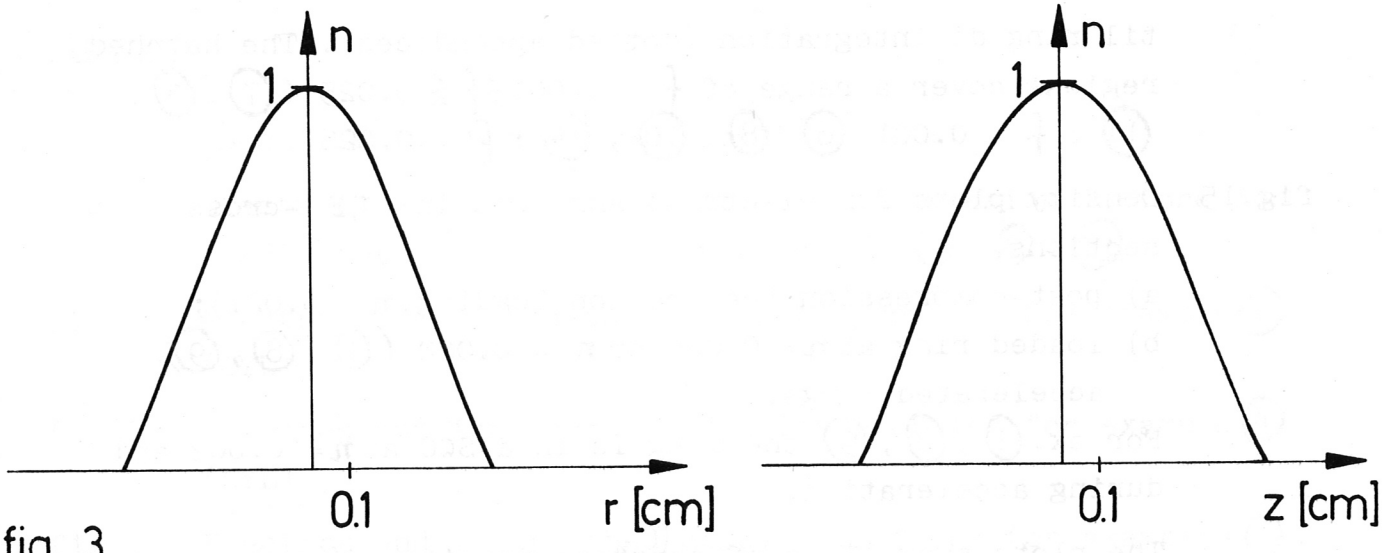

fig. 3

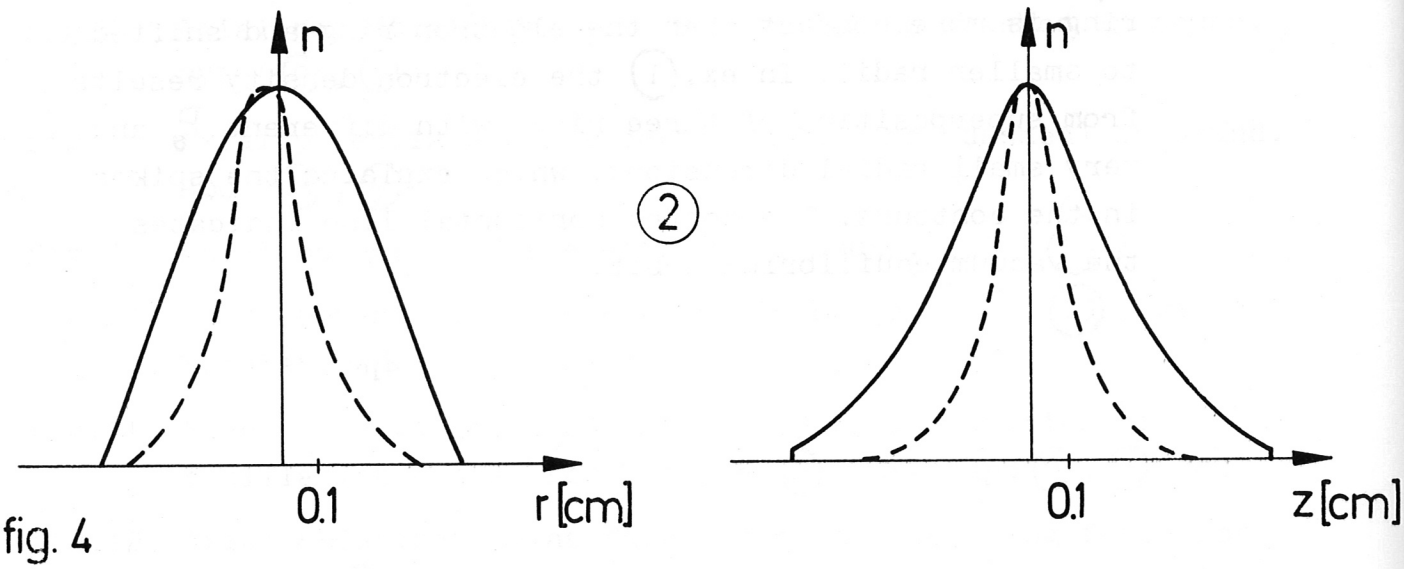

fig. 4

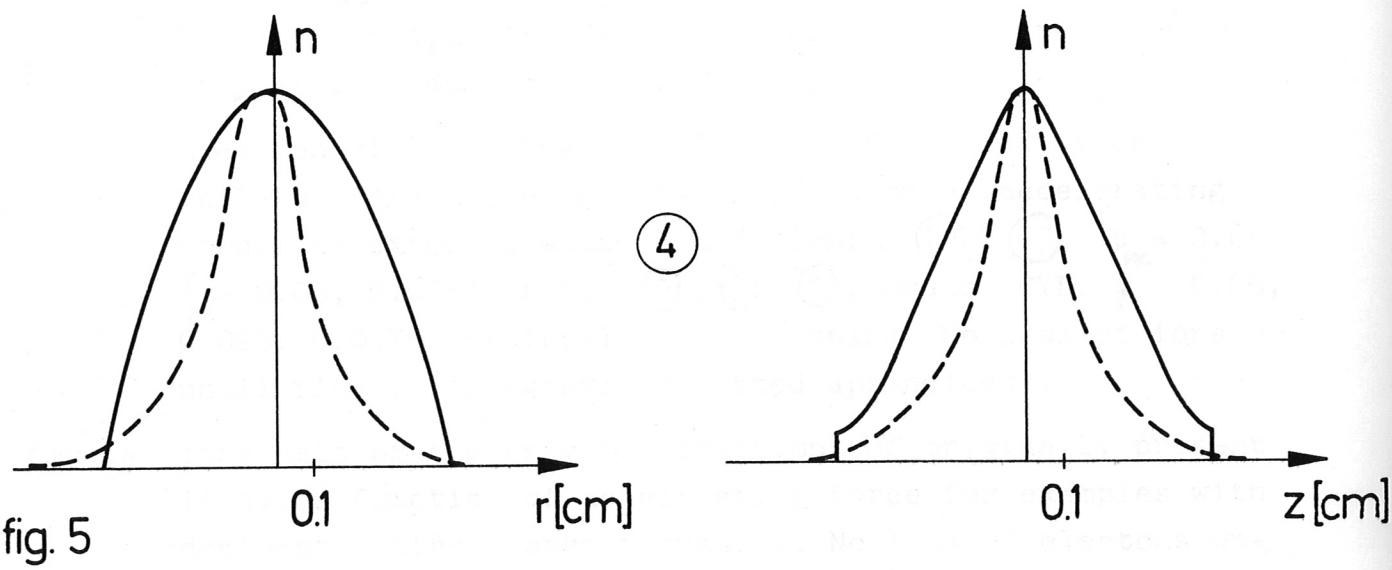

fig. 5

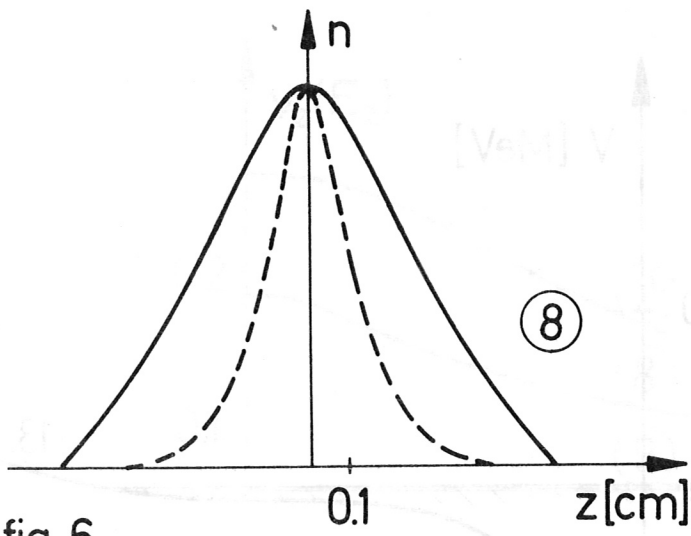

fig. 6

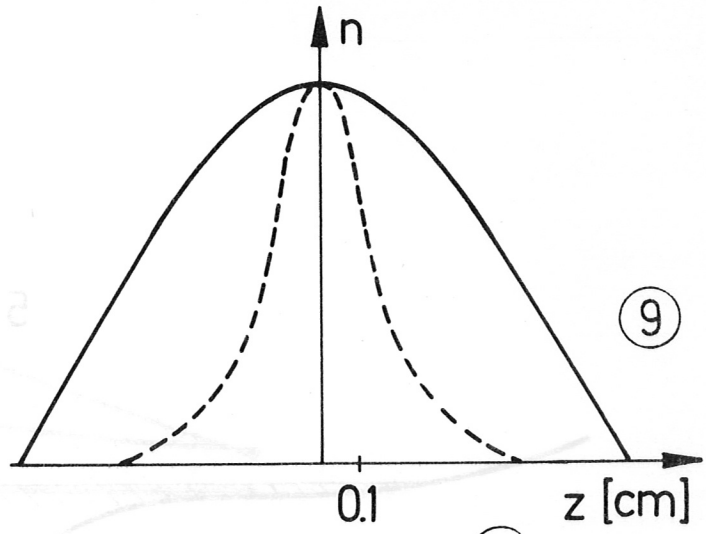

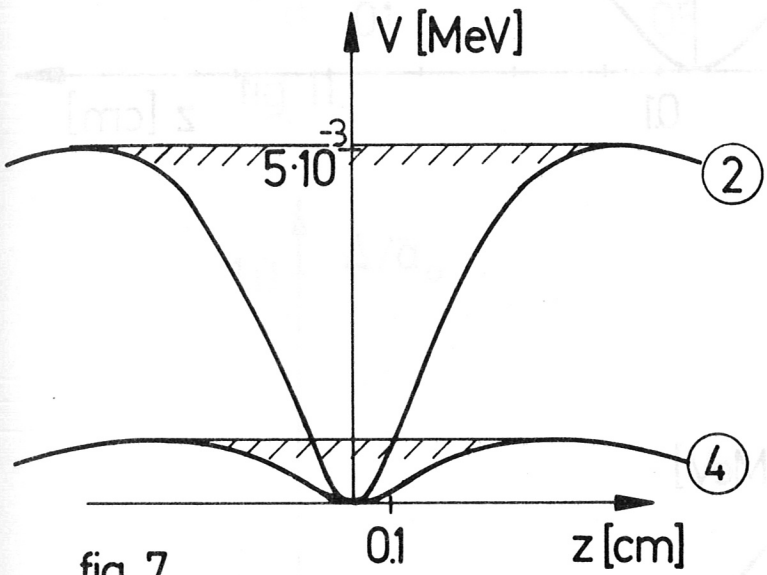

fig. 7

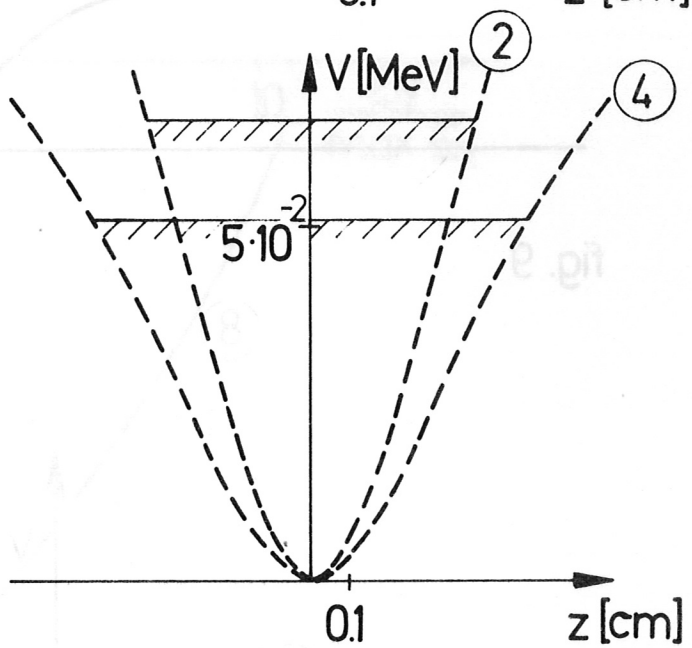

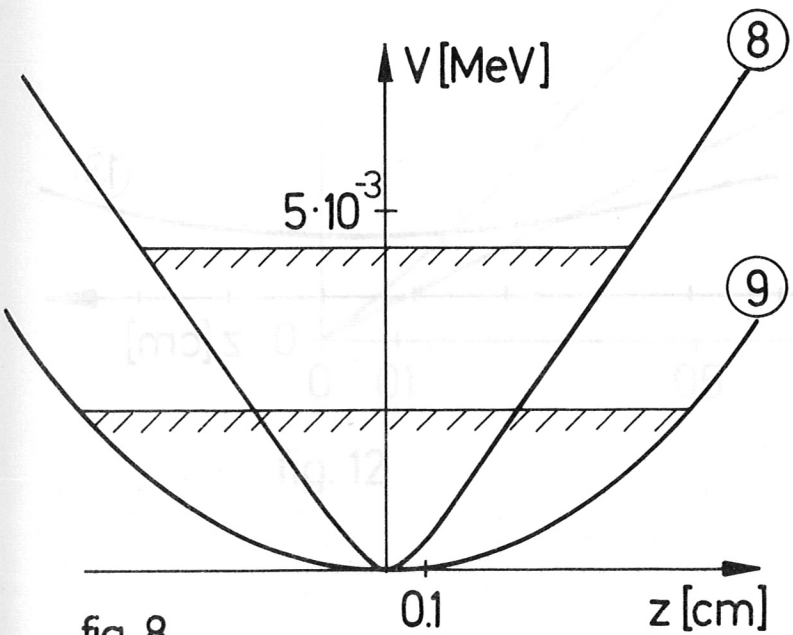

fig. 8

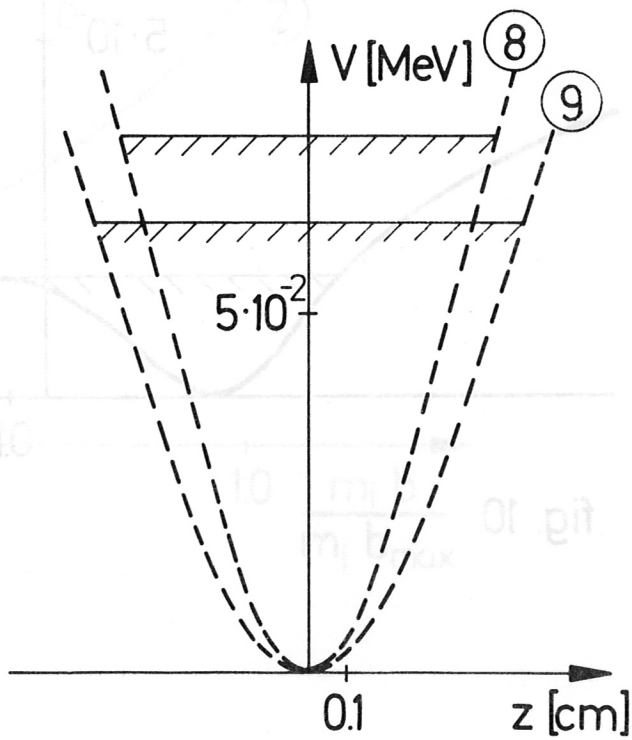

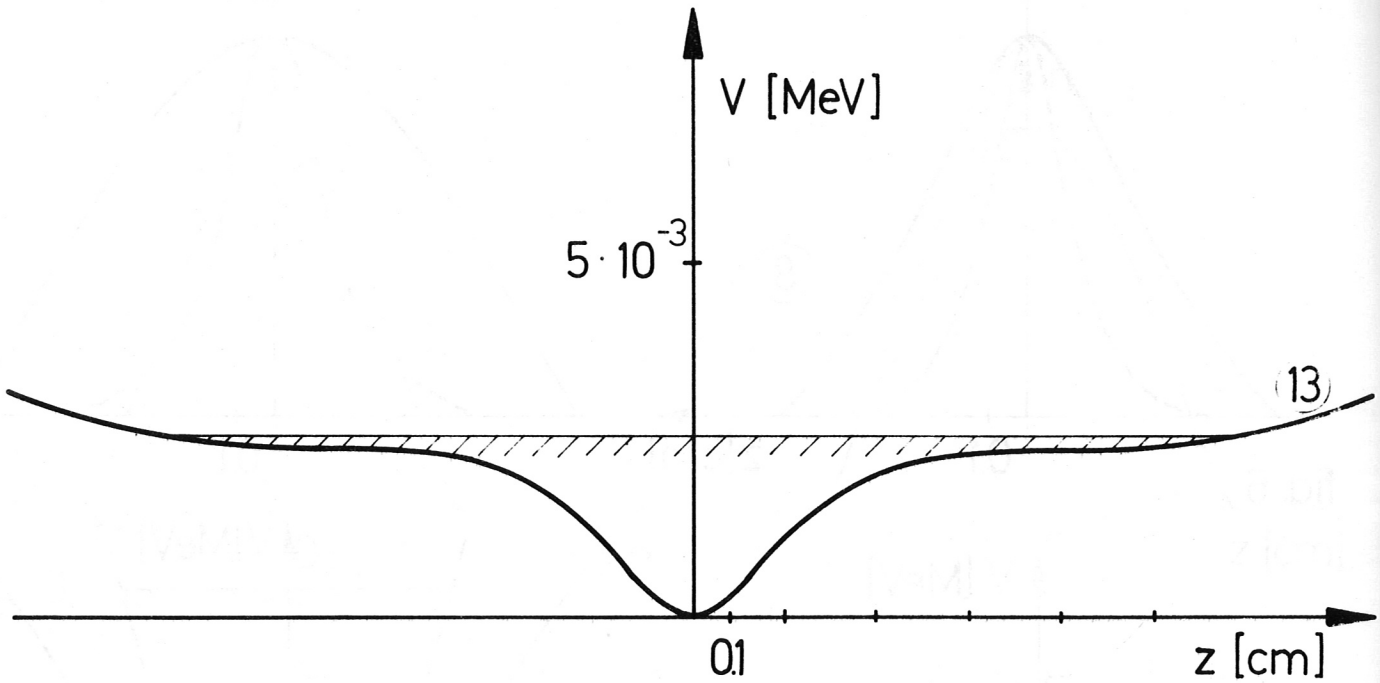

fig. 9

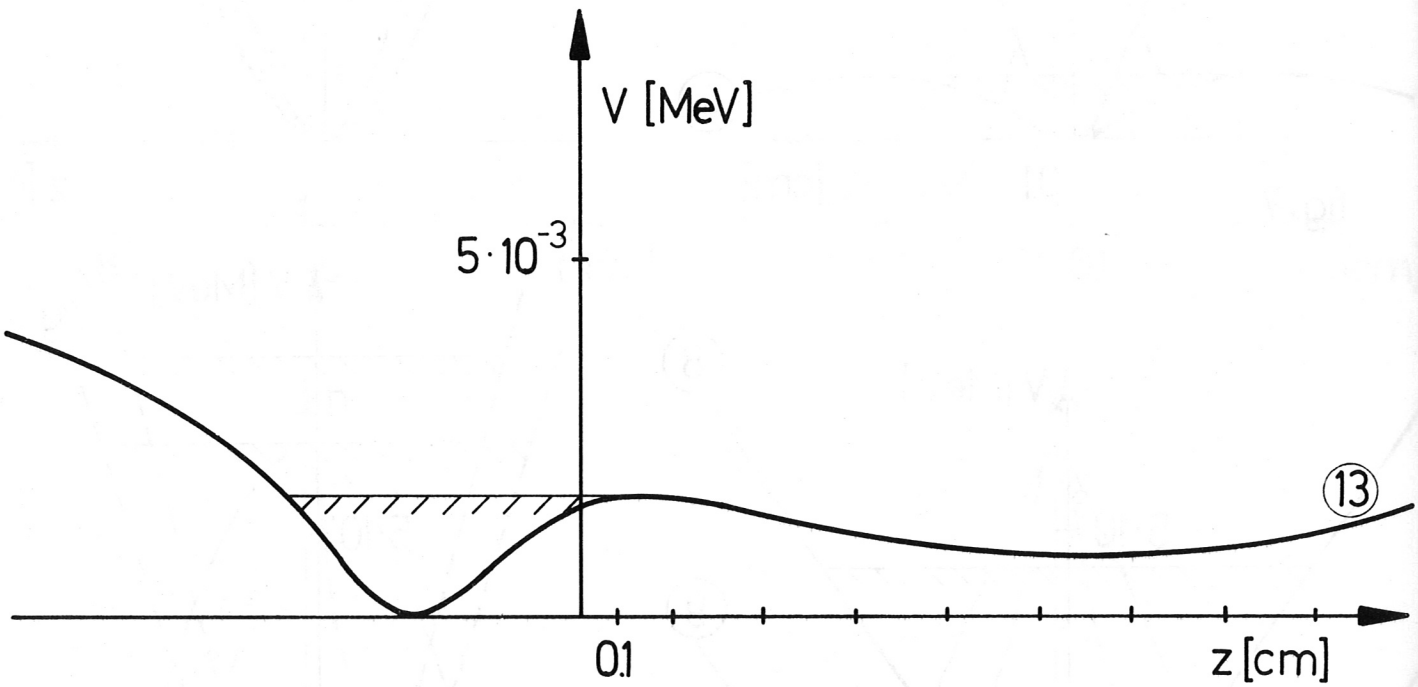

fig. 10

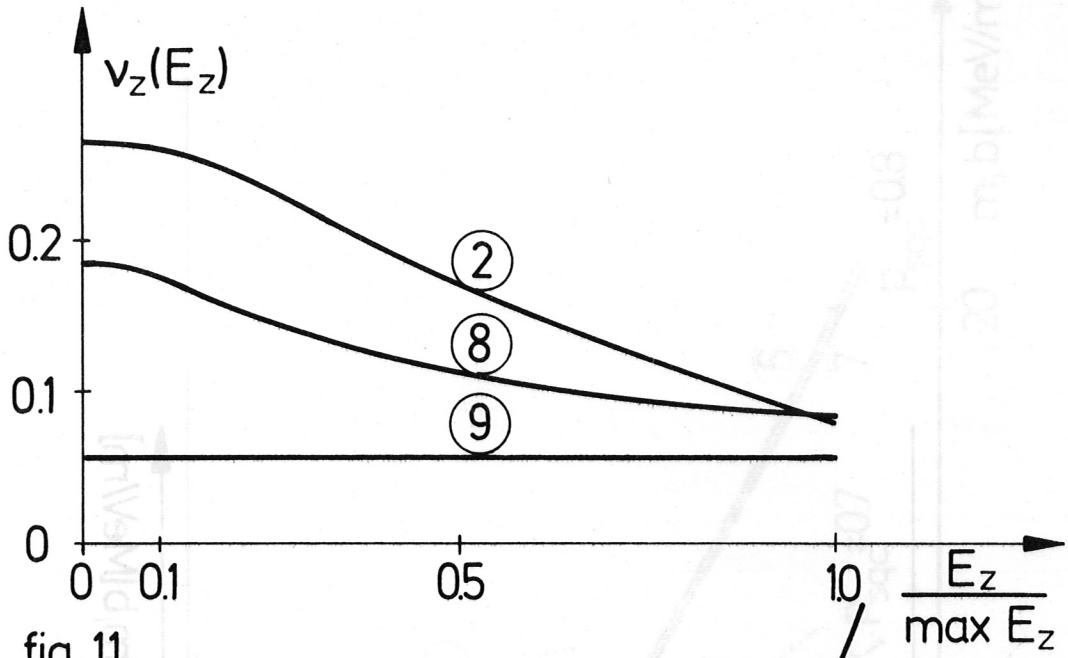
$\nu_z(E_z)$
0.2
0.1
0
2
8
9
0
0.1
0.5
1.0
$\frac{E_z}{\max E_z}$

fig. 11

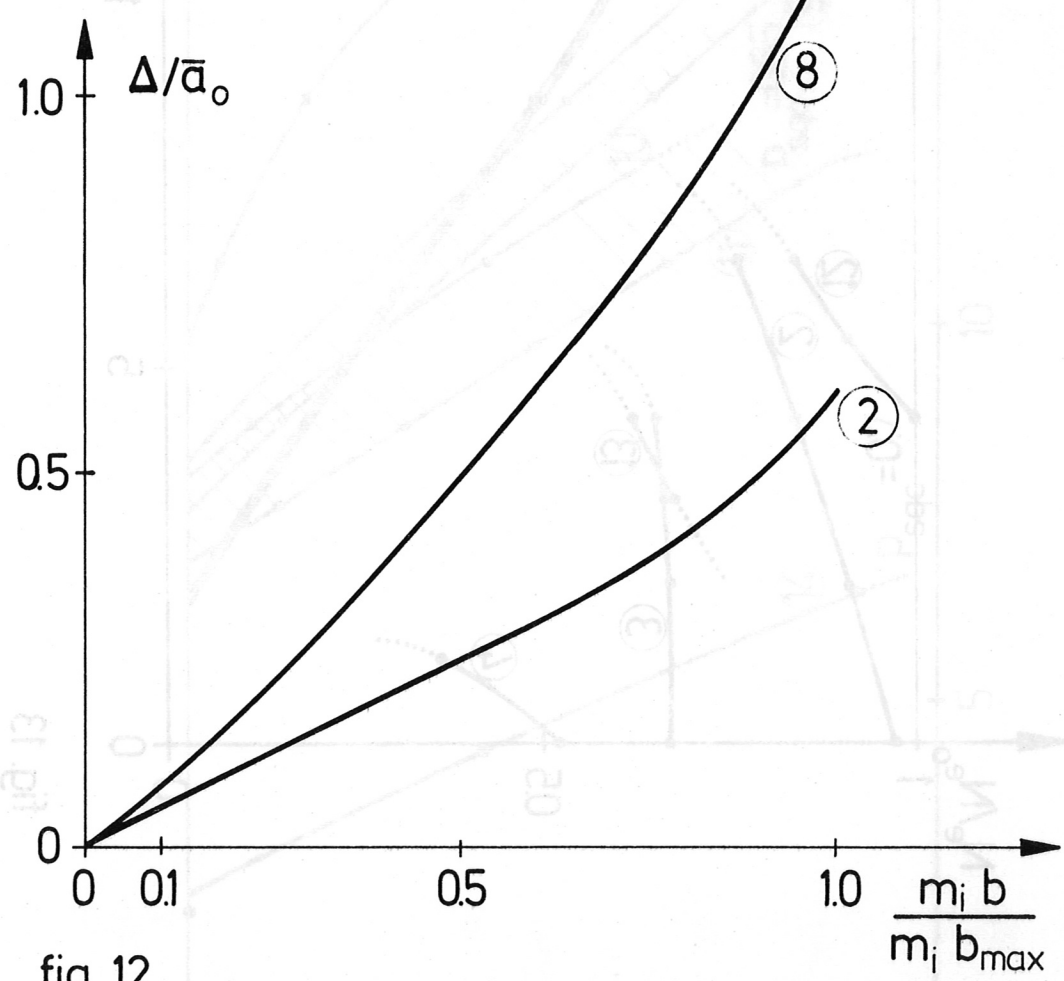
$\Delta/\bar{a}_o$
1.0
0.5
0
8
2
0
0.1
0.5
1.0
$\frac{m_i\, b}{m_i\, b_{max}}$

fig. 12

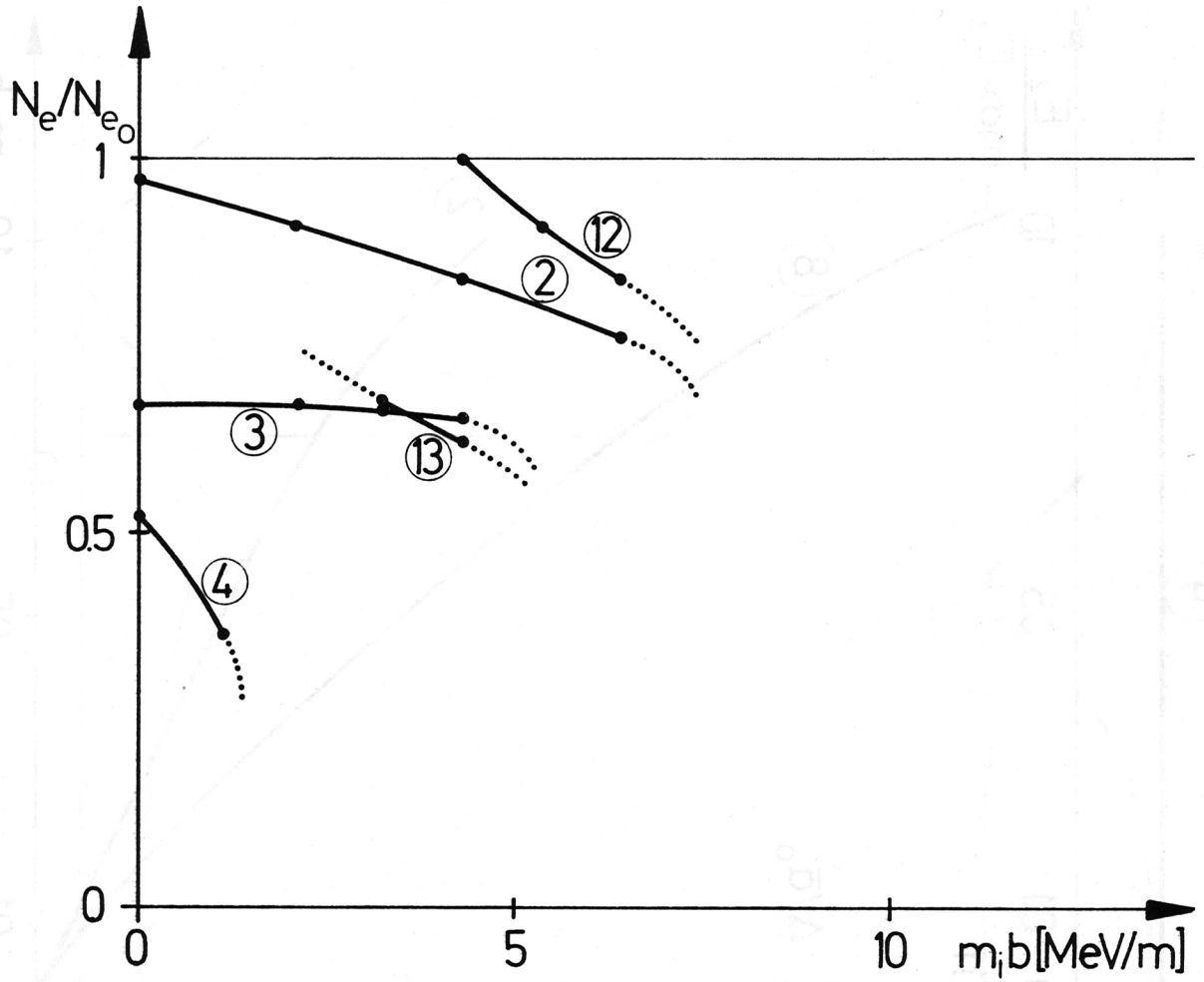

fig. 13

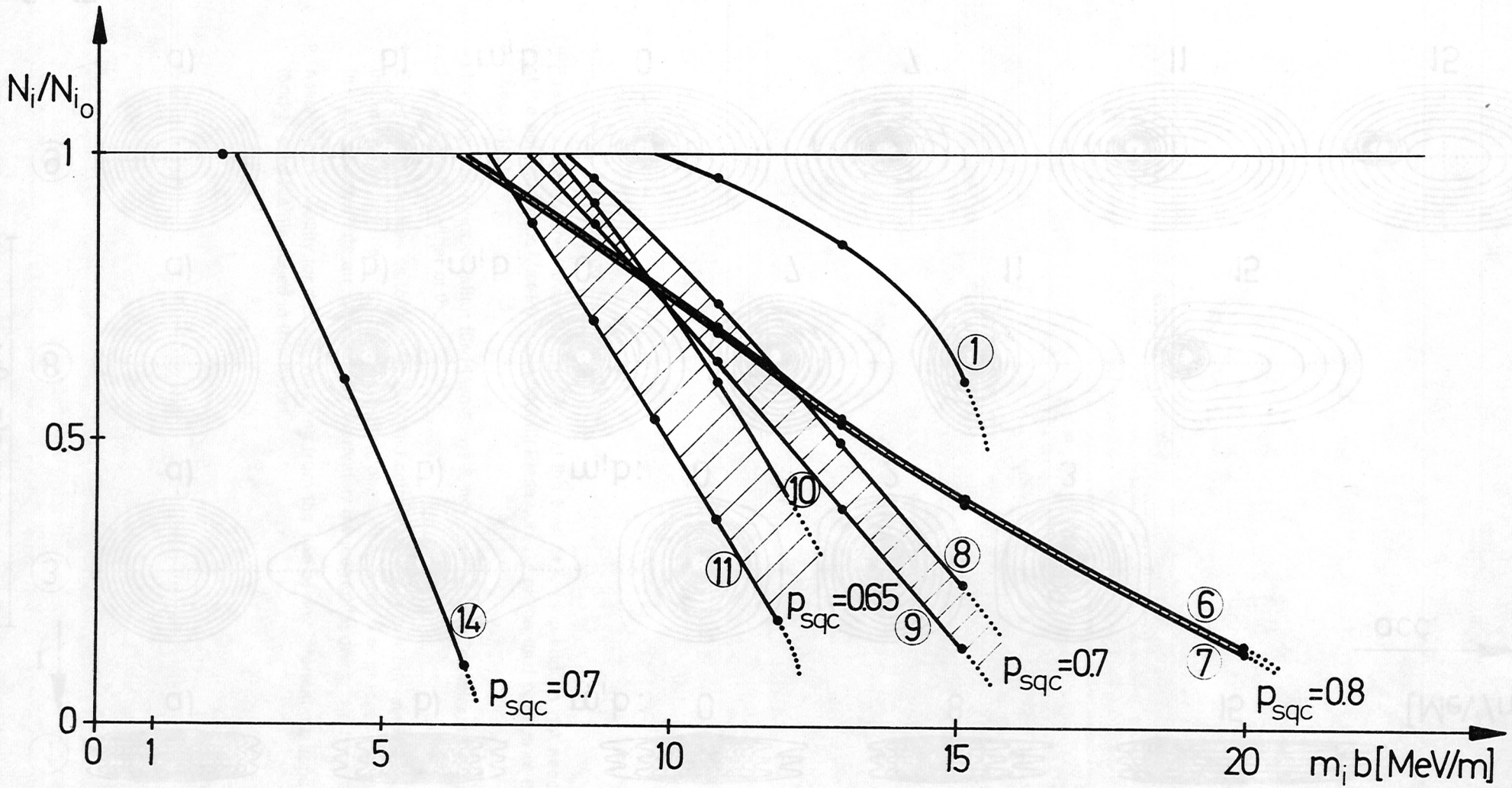
N_i/N_{i_o}
1
0.5
0
0
1
5
10
15
20
m_i b[MeV/m]
1
14
P_{sqc}=0.7
10
11
P_{sqc}=0.65
8
9
P_{sqc}=0.7
6
7
P_{sqc}=0.8

fig. 14

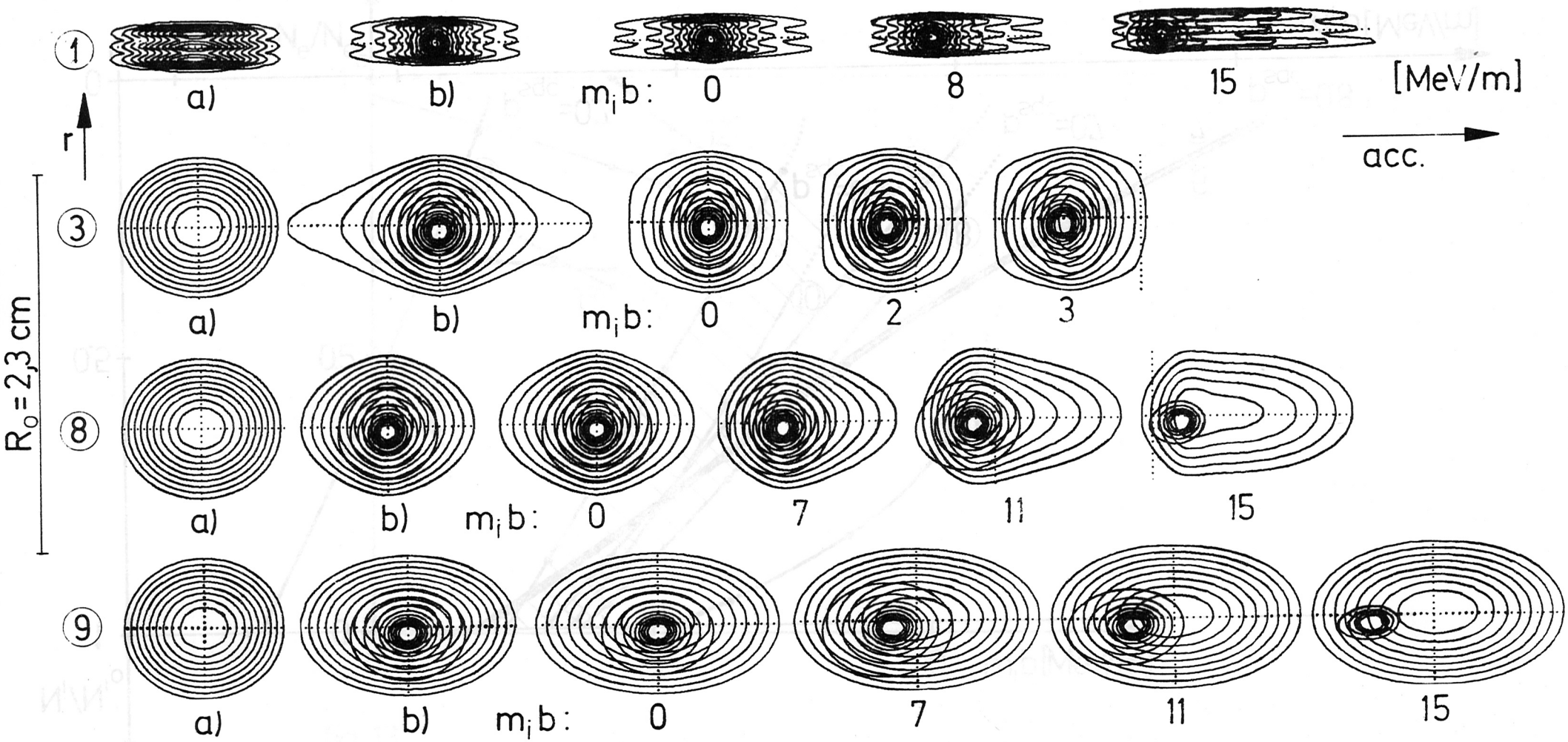
1
a)
b)
$m_i b$: 0
8
15
[MeV/m]
r
acc.
3
a)
b)
$m_i b$: 0
2
3
R_o = 2,3 cm
8
a)
b)
$m_i b$: 0
7
11
15
9
a)
b)
$m_i b$: 0
7
11
15

fig. 15